InteraqCT Comparison on Assemblies - Final Report

Stolfi, Alessandro; De Chiffre, Leonardo

Publication date:
2016

Document Version
Publisher's PDF, also known as Version of record

This project is funded by the European Union

INTERAQCT

DTU

InteraqCT Comparison on Assemblies

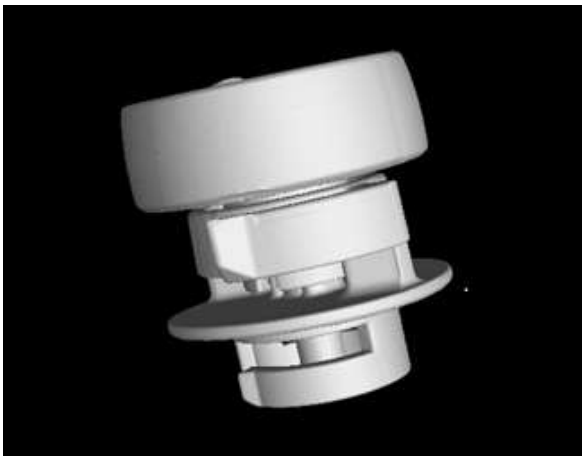

Final report

November 2016

A. Stolfi, L. De Chiffre

Department of Mechanical Engineering

Technical University of Denmark

Table of Contents

Abstract

An interlaboratory comparison on industrial X-ray Computed Tomography (CT) was organized by the Centre for Geometrical Metrology (CGM), Department of Mechanical Engineering, Technical University of Denmark (DTU) and carried as part of the Marie Curie ESR Project INTERAQCT. In the comparison, 22 laboratories from 7 countries were involved, and two assemblies, Assembly 1 and Assembly 2, having different materials and sizes were circulated. Assembly 1 is a physical item while Assembly 2 is a CT scan of industrial assembly. Various measurands are considered, encompassing lengths, diameters, roundness and concentricity. A multi-material length is also included in the comparison. Two different scanning approaches were considered within the comparison exercise for Assembly 1. The first approach, coded as “Own Choice”, does not apply any scanning restrictions on any of the scanning parameters. The second one, coded as “Fast Scan”, introduced a series of limitations, including the scanning time and the number of images per projection.

22 samples of Assembly 1 were circulated in parallel to the participants. A single sample of Assembly 2 was electronically circulated to the participants. The results of each participant are kept confidential. Participants can identify their individual results using an anonymous identification number provided by the coordinator at the beginning of the circulation. All samples were measured by the coordinator using a coordinate measuring machine before and after circulation. The samples of Assembly 1 have shown a good stability over the total comparison time of 8 months. No stability investigation was conducted on Assembly 2 due to the absence of circulation. Depending on the item and measurand, the reference expanded uncertainties (k=2) ranged from 1.1 µm to 2.6 µm.

Participants stated measurement uncertainties in the range between 2 µm and 100 µm for all measurands of Assembly 1. The majority of participants stated measurement uncertainties based on MPE, whereas just a few participants used more complex uncertainty models. The metrological consistency of participants´ results was investigated using the E_n value, where $|E_n| < 1$ indicates agreement between measurement results while $|E_n| \geq 1$ shows disagreement. 71% of the measurements conducted using the Own Choice approach are in agreement with the reference values. 59% of the measurements carried out using the Fast Scan approach are in accordance with the reference values. *L2*, *L3, and T*, which are bidirectional measurands, show lower agreement than *L1* and *L4*, which are unidirectional lengths. The majority of participants obtained similar results in both scanning approaches. A few participants achieved significantly different measurement results, most probably due to the impossibility of selecting suitable scanning parameters. Systematic errors were detected for some participants, especially in CT systems not built for metrology. Results for Assembly 2 showed that increasing the complexity of the measurand increases the range of variation among participants. A good agreement was obtained among

participants for diameters, whereas a worse agreement was registered for roundness and concentricity. It was also observed that participants obtained different results although they used similar inspection software and measuring strategies.

Measuring procedures provided by the coordinator for both assemblies were followed by participants without problems. Most participants carried out measurements and sent their results to the coordinator according to the schedule.

Preface

The InteraqCT comparison on assemblies is as an activity within the Marie Curie ESR Project INTERAQCT - International Network for the Training of Early stage Researchers on Advanced Quality Control by Computed Tomography funded by the European Commission's 7th Framework Programme FP7-PEOPLE - Under grant agreement No 607817. Detailed information is available at http://www.interaqct.eu/.

The project team at DTU Department of Mechanical Engineering, Centre for Geometrical Metrology (CGM) was composed of:

Alessandro Stolfi, Ph.D. Student

Leonardo De Chiffre, Professor

Rene´ Sobieski, Senior metrologist

The participants involved in the comparison were:

3D-CT A/S	Denmark
Carl Zeiss IMT GmbH	Denmark
Danish Technological Institute (DTI)	Denmark
Deggendorf Institute of Technology (DIT)	Germany
Grundfos A/S	Denmark
Federal institute for materials research and testing (BAM)	Germany
Huddersfield University (HUD)	United Kingdom
Katholieke Universiteit Leuven	Belgium
National Physical Laboratory	United Kingdom
Nikon Metrology UK	United Kingdom
Novo Nordisk A/S, Device R&D	Denmark
Novo Nordisk A/S, DMS Metrology & Calibration	Denmark
Nuova Pignone Italia	Italy
Physikalisch-Technische Bundesanstalt (PTB)	Germany
RWTH Aachen	Germany
SIMTech	Singapore
University of Applied Science Upper Austria	Austria
University of Nottingham	United Kingdom
University of Padova (UNIPD)	Italy

Universität Erlangen-Nürnberg (FAU)	Germany
Werth Messtechnik GmbH	Germany
YXLON International GmbH	Denmark

1. Project

The purpose of the comparison was to investigate the performance of industrial Computed Tomography (CT) with respect to dimensional measurements on assemblies. The influence of CT-scanning parameters and post-processing strategies is a topic of interest in this comparison.

The comparison was based on the circulation of two multi-material assemblies. The first item is a physical assembly consists of an aluminum part and a glass part. The item was developed and manufactured in-house. The second item was composed of CT data sets obtained from an industrial assembly with two different polymer parts. The CT data sets feature different noise levels. The second workpiece was provided by Novo Nordisk, a Danish pharmaceutical company.

Different measurands have been selected on the two assemblies to reflect typical industrial applications. A multi-material length was also considered.

The InteraqCT comparison is organized to

- test the applicability of CT for measurement on assemblies with materials and dimensions commonly used in industry;
- evaluate the impact of instrument settings and operator decisions on the measurement of assemblies with two different materials and geometries;
- evaluate the accuracy of CT measurements from Fast Scans;
- investigate the extent to which post-processing settings affect the accuracy of CT measurements.

1.1. Project management and time schedule

The phases involved in the project were:

1. Planning and definition of the participants.
2. Selection of the items and their calibration.
3. Circulation of the items.
4. Analysis of the results.
5. Reporting and dissemination of the results.

Table 1 shows the schedule of the project.

A final workshop to discuss the results of the comparison was held at DTU on September 9th, 2016 (See Figure 1)

Table 1. Time schedule for the InteraqCT comparison.

	2015								2016								
Tasks	5	6	7	8	9	10	11	12	1	2	3	4	5	6	7	8	9
Definition of items and measurands	■																
Manufacture and calibration of items		■	■	■	■	■	■	■									
Circulation of items									■	■							
Re-calibration of items										■	■	■	■	■	■	■	
Reporting												■	■	■	■	■	■

Figure 1. The final workshop of the InteraqCT comparison took place at DTU on the 9th of September 2016. From left, Trine Sørensen (Novo Nordisk A/S, DK), Martin Heath (Werth Messtechnik, DE), Andrew Ramsey (Nikon Metrology, UK), Adam Thompson (University of Nottingham, UK), Jan Lasson Andreasen (Novo Nordisk A/S, DK), Charlotte Haagensen (Novo Nordisk A/S, DK), Rene´ Sobiecki (DTU, DK), Alessandro Stolfi (DTU, DK), Jochen Hiller (Fraunhofer- IIS, DE), Leonardo De Chiffre (DTU, DK), Paras Shah (University of Huddersfield, UK), Maarja-Helena Kallasse (Novo Nordisk A/S, DK), Lars Korner (University of Nottingham, UK), Frank Herold (YXLON, DE), Maria Svendsmark Hansen (Danish Technological Institute, DK), Alexandra Krämer (Karlsruher Institut für Technologie, DE), Bo Nicolajsen (Danish Technological Institute, DK), Wim Dewulf (Katholieke Universiteit Leuven, BE), and Gabriel Probst (Katholieke Universiteit Leuven, BE).

1.2. Participants

A total number of 22 industrial CT scanners from Belgium (1 participant), Denmark (6 participants), Germany (8 participants), Italy (2 participant), Singapore (1 participant), and the UK (4 participants) took part in the comparison. An overview of the participants in alphabetical order is given in **Table 2**. National metrology institutes, manufacturers, universities, research centres, and CT-end users are all represented within the comparison.

Table 2. List of the participants in the circulation in alphabetic order.

Num.	Participant	Country
1	3D-CT A/S	Denmark
2	Carl Zeiss IMT GmbH	Denmark
3	Danish Technological Institute (DTI)	Denmark
4	Deggendorf Institute of Technology (DIT)	Germany
5	GRUNDFOS A/S	Denmark
6	Federal institute for materials research and testing (BAM)	Germany
7	Katholieke Universiteit Leuven	Belgium
8	National Physical Laboratory	United Kingdom
9	Nikon Metrology UK	United Kingdom
10	Novo Nordisk A/S, Device R&D	Denmark
11	Novo Nordisk A/S, DMS Metrology & Calibration	Denmark
12	Nuova Pignone Italia	Italy
13	Physikalisch-Technische Bundesanstalt (PTB)	Germany
14	RWTH Aachen	Germany
15	SIMTech	Singapore
16	University of Applied Science Upper Austria	Austria
17	University of Huddersfield	United Kingdom
18	University of Nottingham	United Kingdom
19	University of Padova (UNIPD)	Italy
20	Universität Erlangen-Nürnberg (FAU)	Germany
21	Werth Messtechnik GmbH	Germany
22	YXLON International GmbH	Germany

1.3. Items

The comparison is based on the circulation of two multi-material assemblies: Assembly 1 and Assembly 2.

Assembly 1 (**Figure 2a**) is a multi-material assembly comprising a cylindrical step gauge made of aluminium and a tube made of glass and two fastening caps. The assembly includes both mono-material measurands such as uni-directional and bidirectional lengths on the gauge and multi-material measurands, defined as the distances between the top of teeth of the gauge and the tube. These measurands can be directly calibrated with tactile CMMs using off-the-shelf probes.

The cylindrical step gauge is 56 mm long with 6 grooves at 3.50 mm steps produced by milling from a 14 mm diameter extruded rod. Machining enabled a suitable surface finish (Ra = 0.40 ± 0.05 µm and Rz = 2.00 ± 0.05 µm), as quantified using a stylus instrument on a set of 5 gauges (λs = 2.5 µm and λc = 0.8 mm, sampling length of 4 mm, and 3 replications per gauge) [4].

The glass was purchased as 1m long tubes and subsequently cut into smaller 55 mm long tubes in-house. The tubes have an outer diameter of 17.5 mm and a wall thickness of approximately 1.2 mm. This was assumed to be sufficient to prevent breakage caused by thermal expansion and contact pressure during handling. The aluminium caps and 10 nylon screws complete the assembly as the fastening system. 4 screws (M3 x 8 mm) constrain the relative displacements between the gauge and the tube, while 6 screws (M2 x 5 mm) constrain the relative rotations. The M2x5 screws push the glass against the step gauge, yielding a more stable connection over time.

Assembly 2 (**Figure 2b**) is a CT scan of an industrial multi-material assembly provided by Novo Nordisk A/S. The inner component is made of polyoxymethylene. The outer component is made of ABS-polycarbonate. Both components are produced via injection molding. Assembly 2 was distributed as 4 CT data sets with two noise levels.

Noise in the data sets was tuned by changing the spot size, the detector calibration, and the number of images per projection. Assembly 2 involves more complex shapes than Assembly 1.

(a)

(b)

Figure 2. (a) Assembly 1 and (b) Assembly 2.

The samples of Assembly 1 have been distributed using a box, as shown in **Figure 3**. Assembly 2 was electronically distributed using a FTP server.

Figure 3. (left) Internal box containing Assembly 1 and (right) external box for storage and transportation of the items.

2. Measurement procedures

The participants were responsible for following the Technical Protocol that contained the measurement procedures and instructions prepared by the project coordinator and that was distributed by email before the item circulation. The protocol includes measurement report documents that should be filled out (the templates shown in the Appendix at the end of this report). Two different scanning approaches were considered within the comparison exercise. The first approach, coded as “Own Choice”, does not present any limitations. The second one, coded as “Fast Scan”, introduced a series of limitations, including the scanning time.

A detailed discussion of the items, measurements details, datum system to be used, and measurands can be found in the [Technical Protocol], and is summarized in Table 3, Table 4, **Figure 4**, and **Figure 5**.

Table 3. Assembly 1 – description of measurands: L1, L2, L3, L4, and $T_{average}$.

Identification	Type of features	Description
L1	Unidirectional Dimension	Distance between flank 7 and flank 9. The distance is measured using two planes (GG). The zone of interest on each flank is shown in figure 5. A number of 20 points distributed over 4 lines were used.
L2	Bidirectional Dimension	Distance between flank 7 and flank 10. The distance is measured using two planes (GG). The zone of interest on each flank is shown in figure 5. A number of 20 points distributed over 4 lines were used.
L3	Bidirectional Dimension	Distance between flank 7 and flank 6. The distance is measured using two planes (GG). The zone of interest on each flank is shown in figure 5. A number of 20 points distributed over 4 lines were used.
L4	Unidirectional Dimension	Distance between flank 7 and flank 3. The distance is measured using two planes (GG). The zone of interest on each flank is shown in figure 5. A number of 20 points distributed over 4 lines were used.
$T_{average}$	Bidirectional Dimension	$T_{average}$ is the average distance between the top of the first tooth and the glass tube along an inspection line of 1.40 mm. There is no constraint regarding the number of distances to be considered.

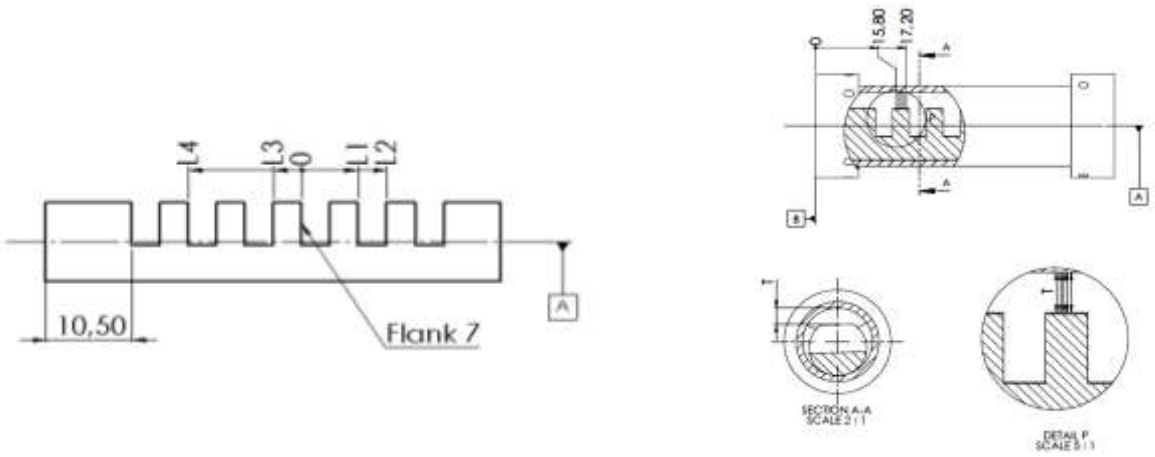

Figure 4. Assembly 1 – Overview of measurands: L1, L2, L3, L4, and Taverage.

Table 4. Assembly 2 – Description of measurands; D1, D2, R1 and C1.

Identification	Type of features	Description
D1	Diameter	Internal diameter, least square fitting (GG) D1 –circle is measured at 2,50 mm from datum B.
D2	Diameter	Outer diameter, least square fitting (GG) D2 –circle is measured at 4,50 mm from datum B.
R1	Roundness	Roundness of the internal diameter D1 (LSCI) without filtering.
C1	Concentricity	Concentricity of the outer diameter D2 (LSCI) with respect to datum A.

Note: (GG = Least Square element as defined in ISO 14405-1 [1]).

Note: (LSCI = Least Square Circle as defined in ISO 12181 [3], [4]).

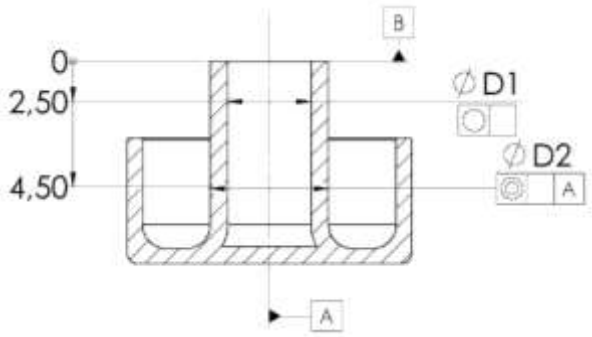

Figure 5. Assembly 2 – Overview of measurands; D1, D2, R2, and C1.

3. Reference values

All the assemblies were measured by the coordinator using a coordinate measuring machine before and after circulation (see **Figure 6**). The coordinate measuring machine was also calibrated, according to VDI/VDE 2617, during the comparison exercise. The calibration procedures are described in detail in [Reference Measurements].

Figure 6. Zeiss UPMC 850 tactile CMM used as calibration equipment within the comparison

Stability of the items was documented through comparison of measurements before and after the circulation. The samples of Assembly 1 have shown a good stability over 8 months.

The calculated reference values and their corresponding uncertainties are shown in **Table 5** and **Table 6** for each sample of Assembly 1 and for the sample of Assembly 2, respectively. The reference values are the average values based on all conducted measurements. The uncertainties represent the biggest values calculated throughout the course of the stability investigation.

Depending on the item and measurand, the reference expanded uncertainties (k=2) ranged from 1.1 µm to 2.6 µm.

Table 5. Assembly 1 – Reference values and their corresponding expanded uncertainties (k=2). Values are in mm.

	L1		L2		L3		L4		$T_{average}$	
No.	**Y [mm]**	**U [mm]**	**Y [mm]**	**U [mm]**	**Y [mm]**	**U [mm]**	**Y [mm]**	**U [mm]**	**Y [mm]**	**U [mm]**
1	7.0012	0.0010	10.5035	0.0015	3.4966	0.0014	13.9991	0.0017	3.5856	0.0024
2	7.0010	0.0012	10.5033	0.0016	3.4970	0.0018	13.9988	0.0019	3.5200	0.0024
3	7.0009	0.0013	10.5040	0.0014	3.4967	0.0015	13.9991	0.0017	3.6629	0.0024
4	7.0004	0.0013	10.5091	0.0017	3.4925	0.0013	13.9992	0.0017	3.5718	0.0026
5	7.0008	0.0013	10.5051	0.0014	3.4957	0.0014	13.9985	0.0015	3.6065	0.0024
6	7.0013	0.0013	10.5115	0.0014	3.4904	0.0013	13.9975	0.0017	3. 6368	0.0026
7	7.0009	0.0013	10.5042	0.0019	3.4952	0.0018	13.9971	0.0017	3.5750	0.0026
8	7.0011	0.0014	10.5053	0.0020	3.4952	0.0018	13.9994	0.0015	3.6613	0.0024
9	7.0015	0.0014	10.5069	0.0019	3.4961	0.0013	13.9995	0.0018	3.6170	0.0024
10	7.0011	0.0015	10.5105	0.0019	3.4872	0.0019	13.9969	0.0017	3.5687	0.0024
11	6.9998	0.0014	10.5129	0.0017	3.4875	0.0019	14.0000	0.0018	3.6097	0.0026
12	7.0005	0.0015	10.5029	0.0018	3.4878	0.0019	14.0005	0.0016	3.5714	0.0023
13	7.0004	0.0014	10.5199	0.0019	3.4869	0.0015	13.9978	0.0020	3.5668	0.0024
14	7.0003	0.0014	10.5108	0.0018	3.4879	0.0015	13.9966	0.0016	3.6690	0.0025
15	7.0009	0.0014	10.5093	0.0019	3.4897	0.0018	13.9990	0.0015	3.5948	0.0024
16	7.0005	0.0013	10.5105	0.0014	3.4906	0.0013	13.9950	0.0018	3.5717	0.0024
17	7.0004	0.0014	10.5049	0.0019	3.4940	0.0015	14.0007	0.0016	3.5916	0.0025
18	7.0009	0.0012	10.5070	0.0018	3.4876	0.0016	13.9976	0.0016	3.5525	0.0024
19	7.0011	0.0014	10.5122	0.0014	3.4866	0.0018	13.9973	0.0016	3.6373	0.0024
20	7.0005	0.0014	10.5124	0.0018	3.4967	0.0016	13.9997	0.0024	3.6375	0.0024
21	7.0006	0.0014	10.5028	0.0015	3.4911	0.0018	13.9989	0.0016	4.8200	0.0024
22	7.0003	0.0013	10.5049	0.0017	3.4960	0.0017	13.9983	0.0012	3.6005	0.0024

Table 6. Assembly 2 – Reference values and their corresponding expanded uncertainties (k=2). Values are in mm.

Measurand	**Y [mm]**	**U [mm]**
D1	3.3012	0.0010
D2	5.5432	0.0010
R1	0.0074	0.0015
C1	0.0093	0.0024

4. Analysis of participants' data

This section presents the measurements obtained by the participants and illustrates their data analyses. Not all participants measured all measurands on both assemblies.

4.1. Measurements carried out by participants

Information on the set-up data is provided in the Measurement Report for each item. The main topics are shown in **Table 7**. An example of measurement report is provided in Appendix.

Table 7. Main subjects in the Measurement Report.

GENERAL INFORMATION
CT SCANNER
SOFTWARE
SETUP AND SCANNING
PROCESSING PARAMETERS
UNCERTAINTY ASSESSMENT
ATTACHMENTS

Participant's results are reported in the following. Analyses were performed for the following subjects:

- Main results for Assembly 1.
- Agreement between participants and reference measurements for Assembly 1.
- Industrial CT scanners used by the participants.
- Software adopted by the participants.
- Assembly 1: Impact of instrument settings and operator.
- Assembly 1: Assembly 1: measurement uncertainties provided by the participants.
- Main results for Assembly 2.

4.2. Main results for Assembly 1 scanned using Own Choice approach

20 participants measured Assembly 1 and the results are shown in **Figure 7**, **Figure 8**, **Figure 9**, **Figure 10**, and **Figure 11** for *L1*, *L2*, *L3*, *L4*, and *T,* respectively.

Figure 7 shows that most of participants are in good agreement with the reference measurements for *L1*. Some participants provided measurement results with deviations smaller than calibration uncertainties. 2 out of 22 participants are not in agreement with the reference values, which could be due to threshold determination and non-corrected voxel and temperature corrections.

The participants stated average expanded uncertainties in the range of 0.002 mm to 0.119 mm, with an average uncertainty of 0.008 mm for *L1*.

Figure 8 shows that 12 of the 22 participants are in good agreement with reference measurements for *L2*, with deviations ranging from -0.006 mm to 0.009 mm. As for *L1*, some participants were able to measure with deviations in the order of the calibration uncertainty of samples. 6 out of 22 participants showed large deviations from the reference values, with deviations up to 0.140 mm. Apart from the possible influence of the factors already described above, an improper qualification of the center of rotation and wider cone angle factors can also be factors that led to the larger deviations found for measurand *L2*. The stability of the datum system may also have contributed to the large deviations because second order errors are of increased importance for this measurand.

The participants stated expanded uncertainties in the range of 0.003 mm to 0.080 mm, with an average uncertainty of 0.016 mm, for *L2*.

Figure 9 shows that 12 of the 22 participants are in good agreement with reference measurements for *L3*, with deviations falling within the stated measurement uncertainties. 7 out of 22 participants provided measurements that are not in agreement with the reference values. The non-conforming participants showed systematic deviations varying from 0.050 mm to 0.126 mm.

The measurement results appeared to be both overestimated and underestimated with respect to the reference values. Such large differences can be due to a post-processing beam hardening correction, which corrupted the real distribution of the grey values, and due to an improper correction of scale error correction.

The participants stated expanded uncertainties in the range of 0.001 mm to 0.080 mm, with an average uncertainty of 0.014 mm, for *L3*.

Figure 10 shows that 20 out of 22 participants are in good agreement with reference measurements for *L4*, with deviations below 0.010 mm. Some participants provided measurement results with deviation in the order of the calibration uncertainty of samples. 2 out 22 participants showed deviation up to 20 µm. Such large differences can be due to a post-processing beam hardening correction, which corrupted the real distribution of grey values, and due to an improper correction of scale error correction. The stability of datum system may also have had an effect on the big deviations because second order errors gain in importance.

The participants declared expanded uncertainties in the range of 0.002 mm to 0.080 mm, with an average uncertainty of 0.014 µm, for *L4*.

Figure 11 highlights that 11 participants are in good agreement with reference measurements, with deviations lying within the stated measurement uncertainties. It is interesting to note that although *T* and the length *L3* are similar, both are bi-directional length of similar size, the deviations registered for T are larger than those observed for *L3*. This result confirms the greater difficulty in defining a multi-material surface determination and a stable datum system for measurements of *T* compared to *L3*. 4 out of 22 participants showed measurements results that are not in agreement with reference measurements, with an average deviation of 0.057 mm.

The participants declared expanded uncertainties for *T* in the range of 0.002 mm to 0.080 mm, with an average uncertainty of 0.014 mm. The uncertainty measurements stated for *T* are equal to the ones stated for *L3*.

Table 8 reports the deviation-to-voxel-size ratios for all measurands to better demonstrate the extent of the measurement errors. The length measurements *L1* show an average ratio of 11 % with a maximum value of 124 % and a minimum value of 0.2 %. The length measurements of *L2* show a mean ratio of 36 % with a maximum value of 245 % and a minimum value of 0.1 %. The length measurements for *L3* present an average ratio of 29 % with a maximum value of 195 % and a lowest value of 0.2 %. The length measurements of *L4* show a ratio of 20 % with a maximum value of 183 % and a minimum value of 0.1%. The length measurements of *T* have a ratio of 34 % with a maximum value of 115 % and a minimum value of 2 %.

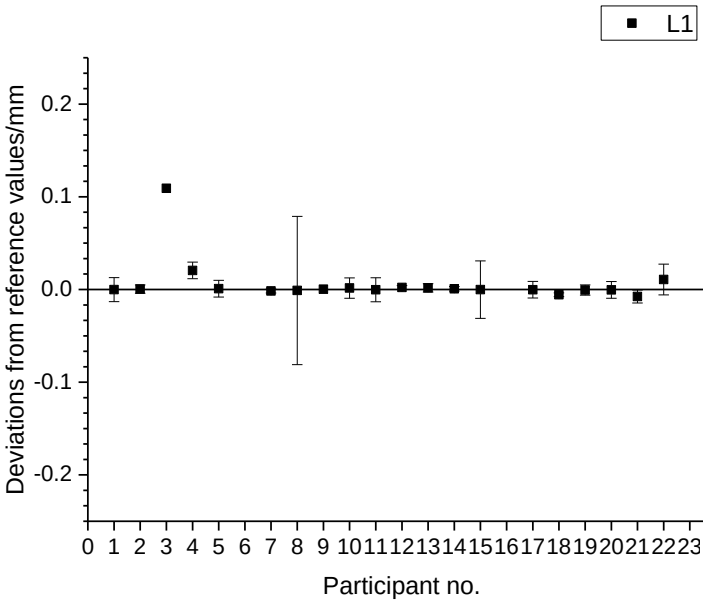

(a)

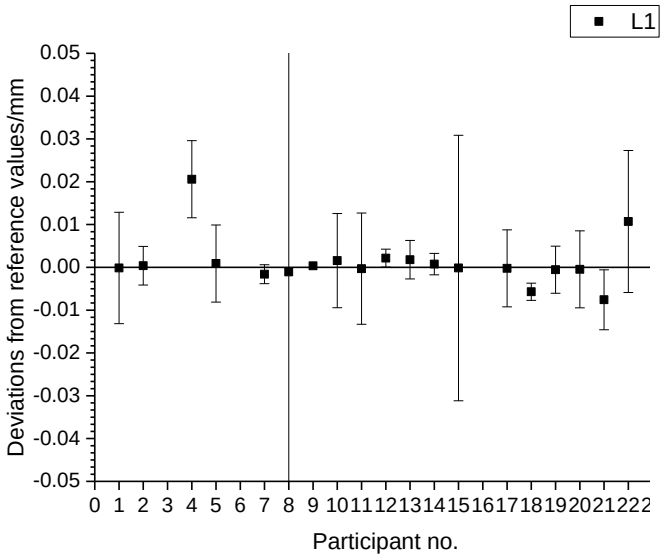

(b)

Figure 7. Results for Assembly 1. Length L1: (a) deviation range ± 0.25 mm, (b) deviation range ± 0.05 mm

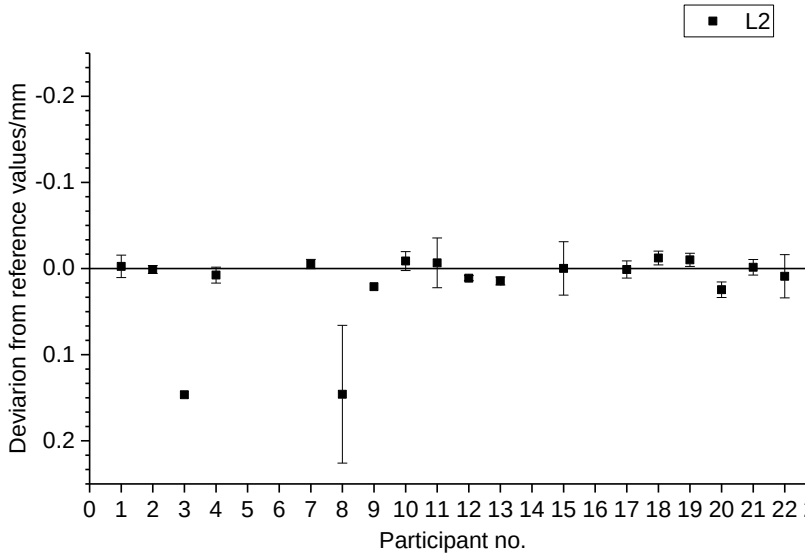

(a)

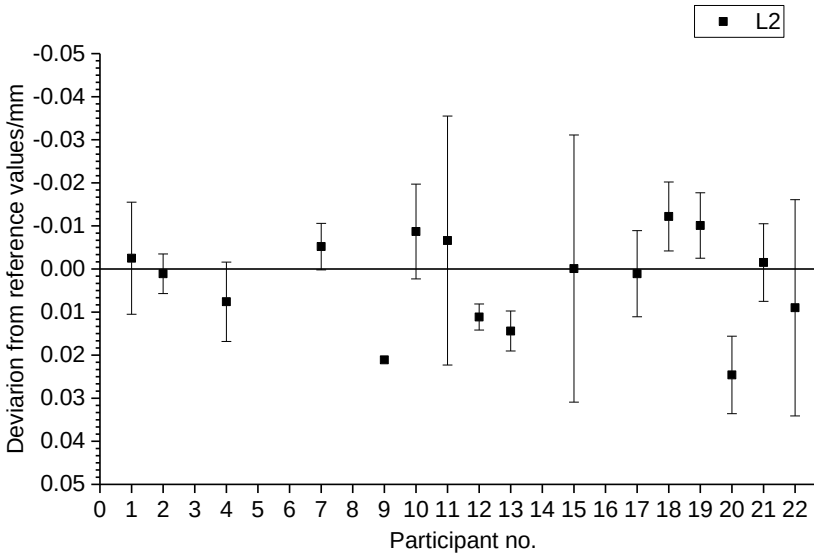

(b)

Figure 8. Results for Assembly 1. Length L2: (a) deviation range ± 0.25 mm, (b) deviation range ± 0.05 mm

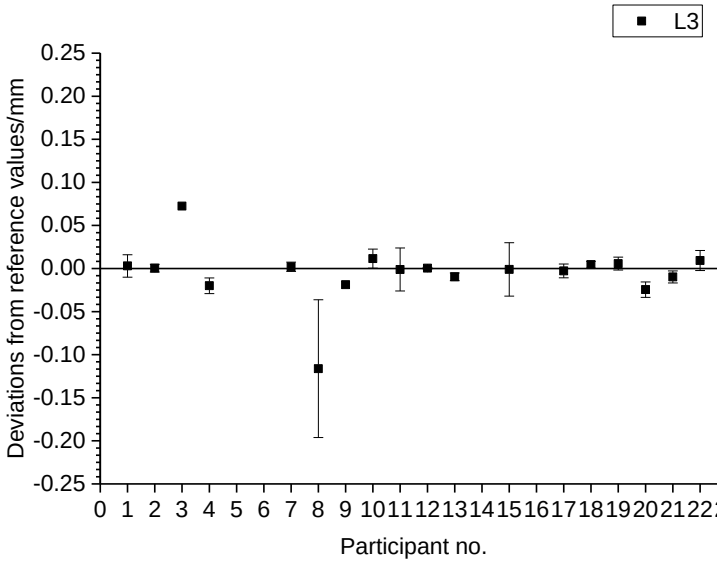

(a)

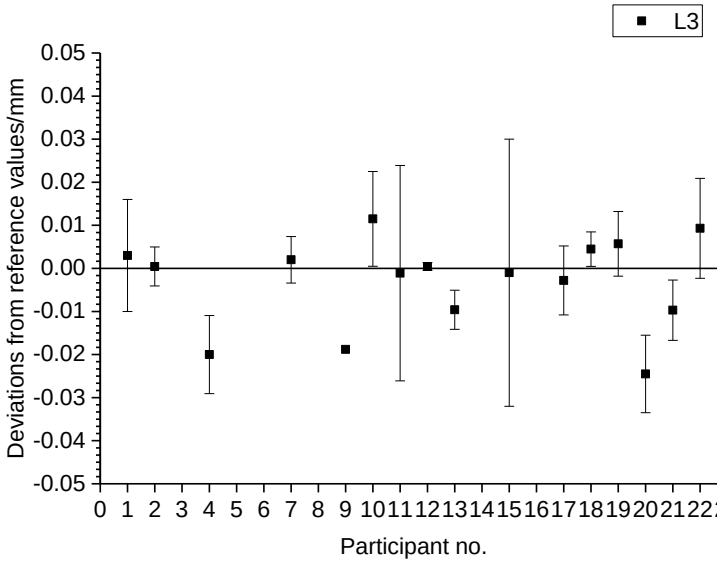

(b)

Figure 9. Results for Assembly 1. Length L3: (a) deviation range ± 0.25 mm, (b) deviation range ± 0.05 mm

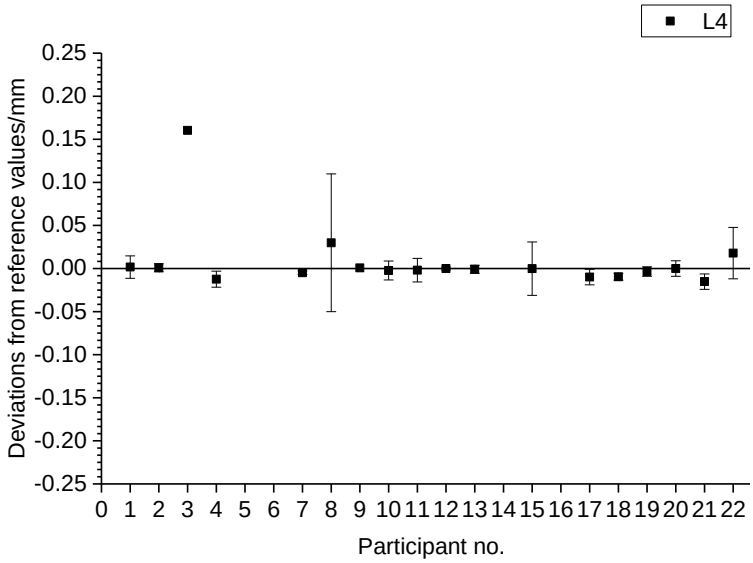

(a)

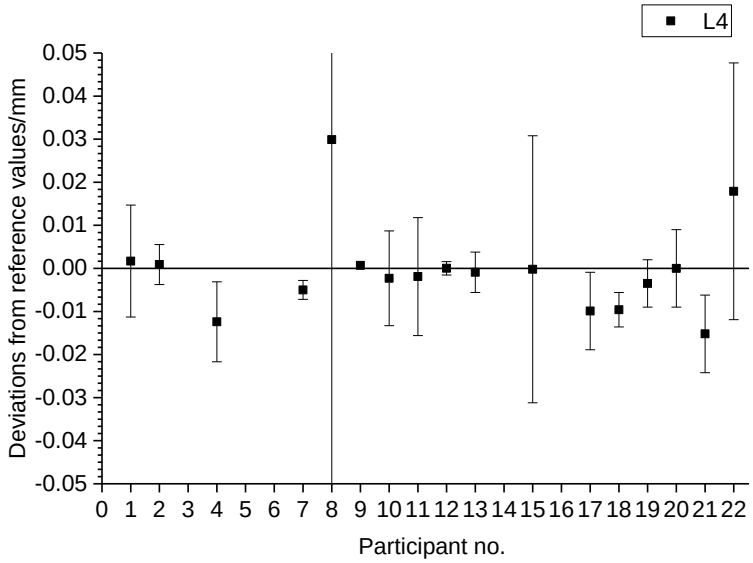

(b)

Figure 10. Results for Assembly 1. Length L4: (a) deviation range ± 0.25 mm, (b) deviation range ± 0.05 mm

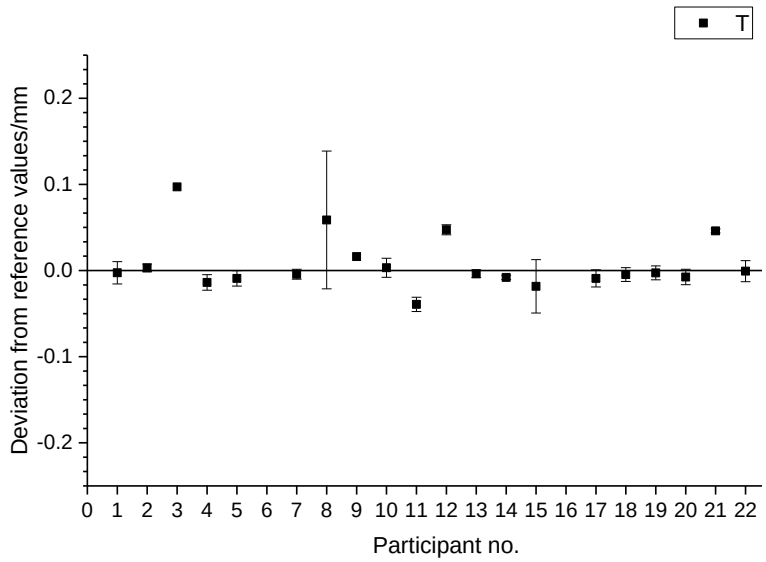

(a)

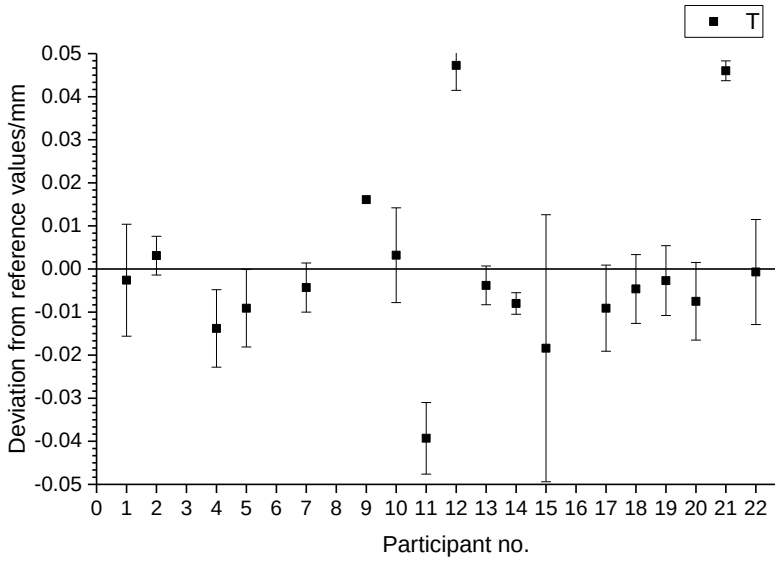

(b)

Figure 11. Results for Assembly 1. Length $T_{average}$: (a) deviation range ± 0.25 mm, (b) deviation range ± 0.05 mm

Table 8. Mean error-to-voxel size ratios (%) for Assembly 1 scanned using the Own Choice approach.

Participant no.	L1	L2	L3	L4	$T_{average}$
1	1	7	5	4	5
2	1	1	2	1	7
3	124	83	166	183	110
4	31	31	9	18	21
5	3	3	4	9	26
6					
7	5	8	18	10	13
8	2	195	245	52	99
9	1	28	29	1	25
10	4	31	27	7	8
11	1	3	19	7	111
12	5	0	24	3	113
13	2	9	13	0	4
14	2	31	33	1	17
15	0	1	1	0	21
16					
17	0	2	0	12	9
18	7	5	14	13	6
19	1	16	25	3	7
20	2	79	49	2	25
21	19	13	5	40	115
22	27	26	19	48	2

4.3. Main results for Assembly 1 scanned using Fast Scan approach

The results are shown for *L1*, *L2*, *L3*, *L4*, and *T* **Figure 12**, **Figure 13**, **Figure 14**, **Figure 15**, and **Figure 16**, respectively.

Figure 12 shows that 14 out of 22 participants are in good agreement with the reference measurements for *L1*, with deviations below 0.097 mm. Some participants provided measurement results with deviations smaller than calibration uncertainty. 2 out of 22 participants showed deviations up to 0.020 mm. The participants stated average expanded uncertainties in the range of 0.001 mm to 0.110 mm, with an average uncertainty of 0.022 mm, for *L1*.

Figure 13 shows a good agreement among 13 participants and the calibration measurements for *L2*, with deviations ranging from –0.006 mm to 0.009 mm. Some of those participants were also able to measure with deviations within the calibration uncertainties. The participants stated average expanded uncertainties in the range of 0.002 mm to 0.110 mm, with an average uncertainty of 0.020 mm, for *L2*.

Figure 14 shows that 13 out of 22 participants are in good agreement with reference measurements for *L3*, with deviations ranging from –0.006 mm to 0.009 mm. Some participants were able to measure with deviations in the order of the calibration uncertainty of samples. The participants stated average expanded uncertainties in the range of 0.002 mm to 0.110 mm, with an average uncertainty of 0.020 mm, for *L3*.

Figure 15 depicts that 18 out of 22 participants are in good agreement with the reference measurements for *L4*, with deviations below 0.01 mm. Some participants provided measurement results with deviation in the order of the calibration uncertainty of the samples. 2 out of 22 participants showed deviation up to 0.020 mm. Such large differences can be due to a post-processing beam hardening correction, which corrupted the real distribution of the grey values, and due to an improper correction of scale error correction. The participants stated average expanded uncertainties in the range of 0.001 mm to 0.110 mm, with an average uncertainty of 0.019 mm, for *L4*.

Figure 16 highlights that participants are in good agreement with reference measurements for *T*, with deviations lying within the stated measurement uncertainties. 4 out 22 participants showed measurements results which are not in agreement with reference measurements, with an average deviation of 0.057 mm. These large deviations may be due to errors in defining the datum system and surface around both materials. The participants declared expanded uncertainties for *T* in the range of 0.002 mm to 0.110 mm, with an average uncertainty of 0.019 mm.

Table 9 lists the deviation-to-voxel-size ratios for all measurands. The length measurements *L1* show a ratio of 19% with a maximum value of 169% and a lowest value of 0.3%. The length measurements of *L2* show a ratio of 34% with a maximum value of 212% and a minimum value of 0.5%. The length measurements of *L3* show a ratio of 50% with a maximum value of 366% and a minimum value 1.2%. The length measurements of *L4* show a ratio of 26% with a maximum value of 252% and a minimum value of 0.5%. The length measurements of *T* show a ratio of 37% with a maximum value of 145% and a minimum value of 3%.

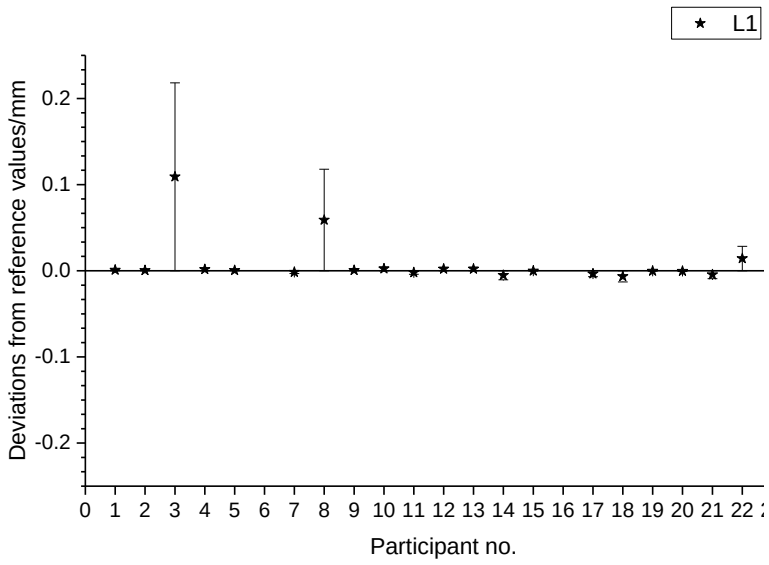

(a)

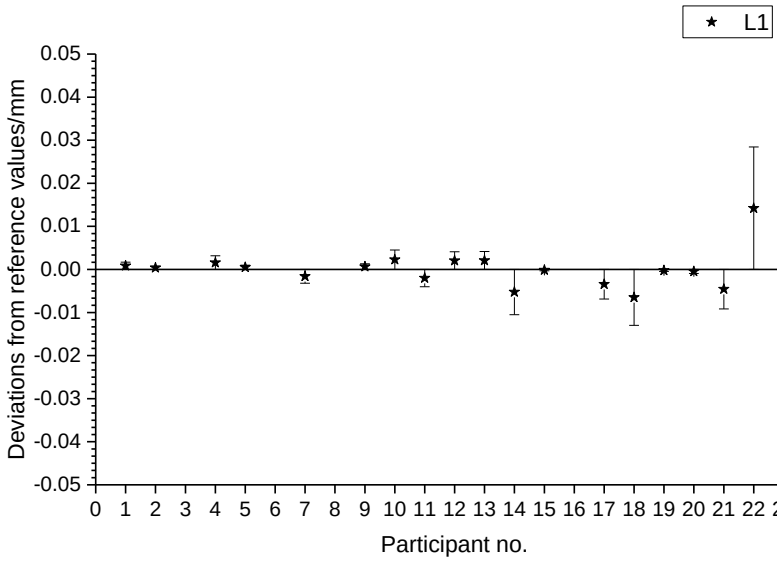

(b)

Figure 12. Results for Assembly 1. Length L1: (a) deviation range ± 0.25 mm, (b) deviation range ± 0.05 mm

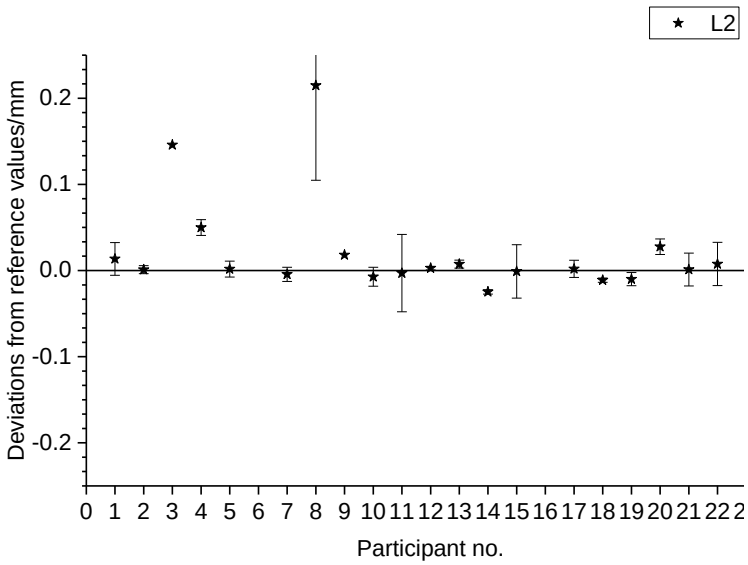

(a)

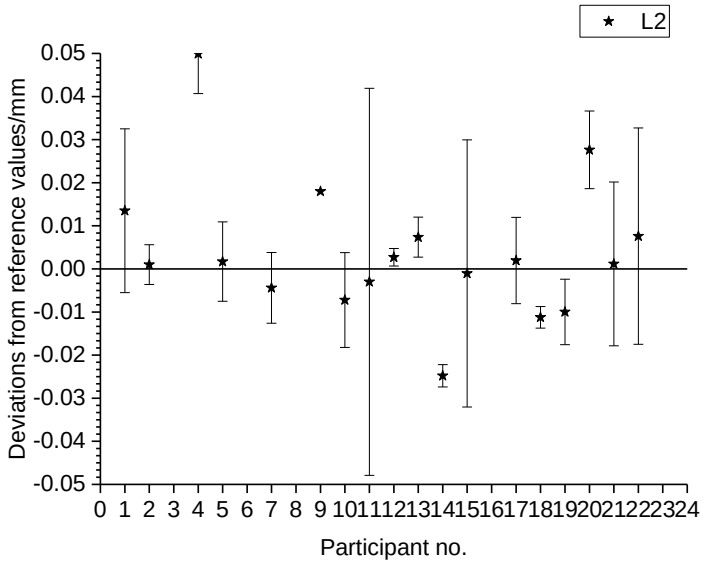

(b)

Figure 13. Results for Assembly 1. Length L2: (a) deviation range ± 0.25 mm, (b) deviation range ± 0.05 mm

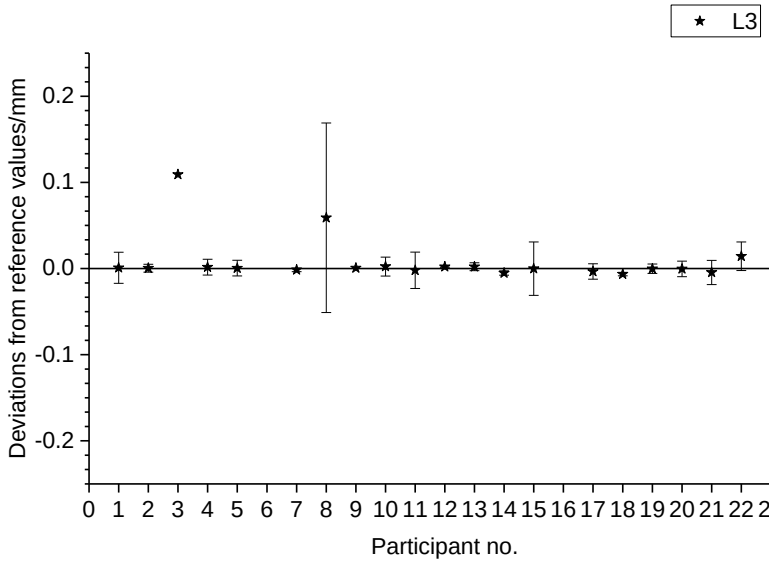

(a)

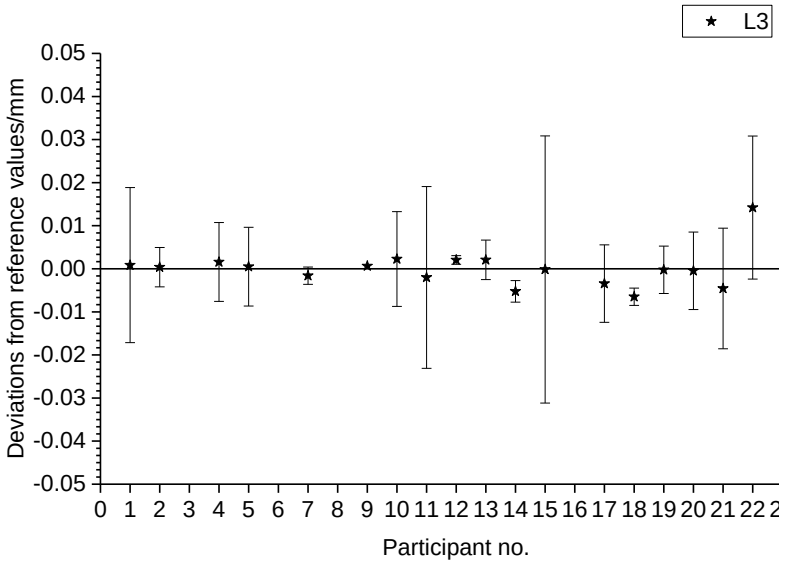

(b)

Figure 14. Results for Assembly 1. Length L3: (a) deviation range ± 0.25 mm, (b) deviation range ± 0.05 mm

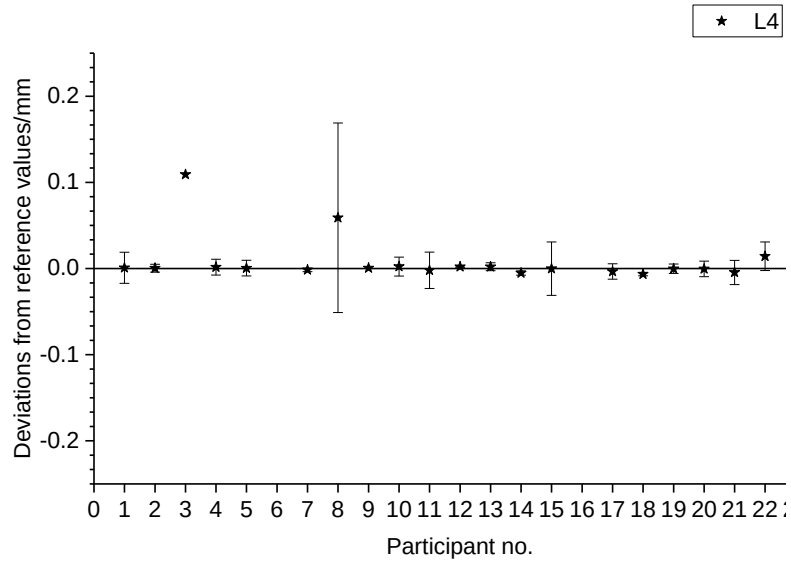

(a)

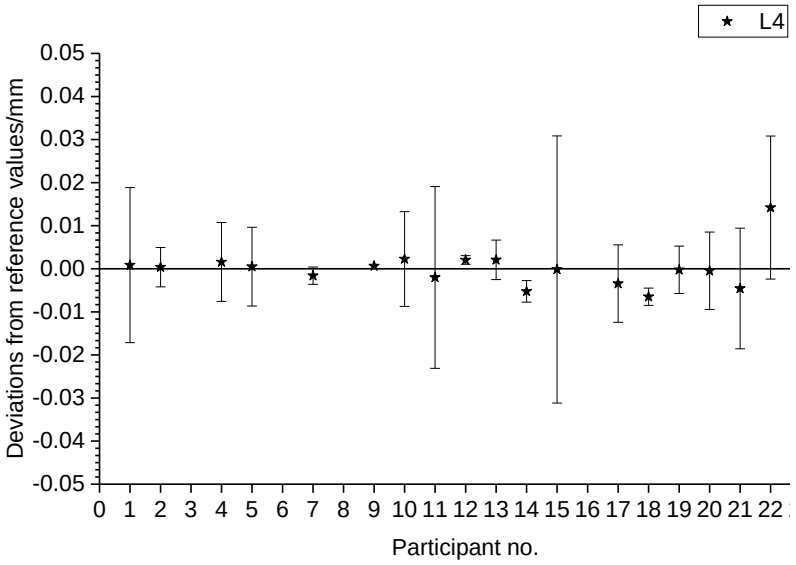

(b)

Figure 15. Results for Assembly 1. Length L4: (a) deviation range ± 0.25 mm, (b) deviation range ± 0.05 mm

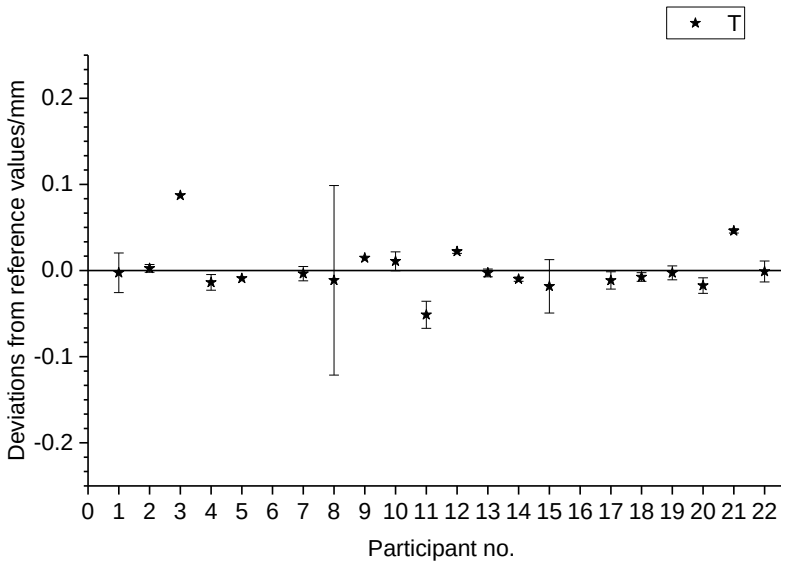

(a)

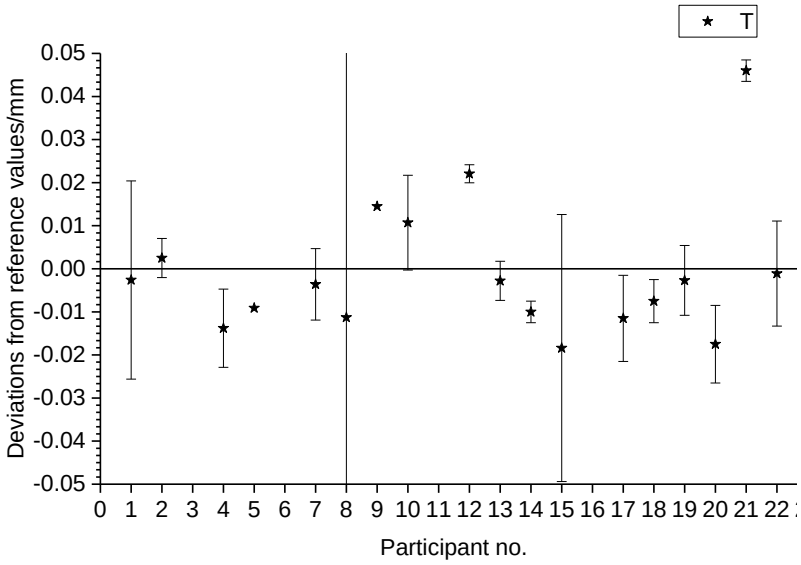

(b)

Figure 16. Results for Assembly 1. Length $T_{average}$: (a) deviation range ± 0.25 mm, (b) deviation range ± 0.05 mm

Table 9. Mean error-to-voxel size ratios (%) for Assembly 1 scanned using the Fast Scan approach.

Participant no.	*L1*	*L2*	*L3*	*L4*	*T*
1	2	23	27	4	5
2	1	1	2	1	5
3	170	130	228	251	136
4	2	7	74	18	21
5	1	4	5	10	26
6					
7	5	3	13	9	11
8	100	212	364	86	19
9	1	33	28	0	23
10	6	18	18	5	27
11	6	3	8	1	145
12	5	18	6	2	53
13	2	9	7	0	3
14	11	33	52	1	21
15	0	1	1	0	21
16					
17	8	4	4	29	25
18	8	6	14	12	10
19	1	17	27	3	7
20	2	122	92	1	58
21	11	8	3	22	115
22	36	35	19	59	3

4.4. Comparison between Own Choice and Fast Scan

Figure 17 shows the deviations between two scanning approaches for all measurands. The deviation, δ, is defined for each measurement as follows:

$$\delta = \mathrm{X}_{\mathrm{Fast-scan}} - \mathrm{X}_{\mathrm{Own-choice}}. \quad (1)$$

Here, $\mathrm{X}_{\mathrm{Fast-scan}}$ is the measurement obtained using the Fast Scan approach and $\mathrm{X}_{\mathrm{own-choice}}$ is the measurement obtained using the Own Choice approach.

The measurements of *L1* show positive average deviations in the order of 0.002 mm, with a maximum deviation between the two approaches of 0.060 mm. The measurements of *L2* show positive average deviations in the order of 0.007 mm, with a maximum deviation between the two approaches of 0.070 mm. Participant no. *1*, *3*, and *8* show the biggest differences for this measurand. The results associated with *L3* show average deviations in the order of -0.001 mm, with a maximum deviation between the two approaches of 0.016 mm. The measurement results related to *L4* present average deviations in the order of 0.002 mm, with a maximum deviation between the two approaches smaller than 0.020 mm. Measurement deviations in the order of -0.005 mm, with a maximum deviation between the two approaches of -0.070 mm, are finally observed for *T*. The majority of participants overestimated the measurement results of *L1*, *L2*, *L3*, and *L4*, and underestimated the measurement values of *T*.

Statistical analysis conducted on measurement results highlighted that number of outliers is larger in the Fast Scan approach than Own Choice approach.

13 out of 22 participants declared similar measurement uncertainties for both scanning approaches, whereas 7 out of 22 participants stated different uncertainty statements. Measurement uncertainties up to 111% larger were provided for Fast-Scan-based measurements compared to the Own-Choice-based measurements.

It can be concluded that the majority participants stated similar both measurement results and measurement uncertainties using both scanning approaches. Just a few participants achieved significantly different measurement results, most probably due to the impossibility of selecting suitable scanning parameters.

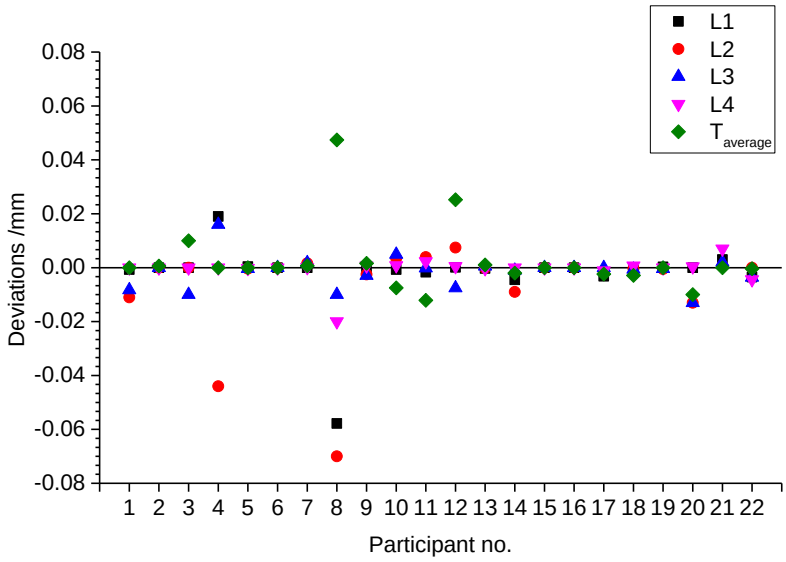
L1
L2
L3
L4
T average
Deviations /mm
0.08
0.06
0.04
0.02
0.00
-0.02
-0.04
-0.06
-0.08
1 2 3 4 5 6 7 8 9 10 11 12 13 14 15 16 17 18 19 20 21 22
Participant no.

(a)

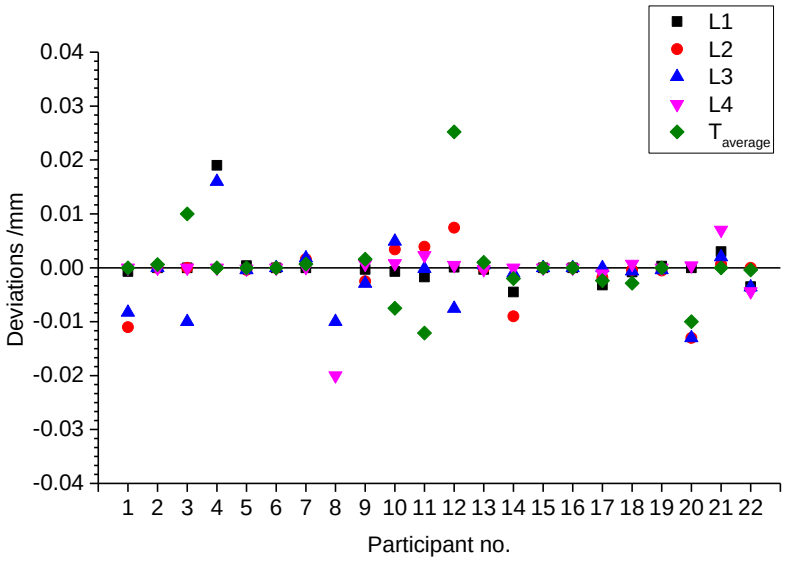
L1
L2
L3
L4
T average
Deviations /mm
0.04
0.03
0.02
0.01
0.00
-0.01
-0.02
-0.03
-0.04
1 2 3 4 5 6 7 8 9 10 11 12 13 14 15 16 17 18 19 20 21 22
Participant no.

(b)

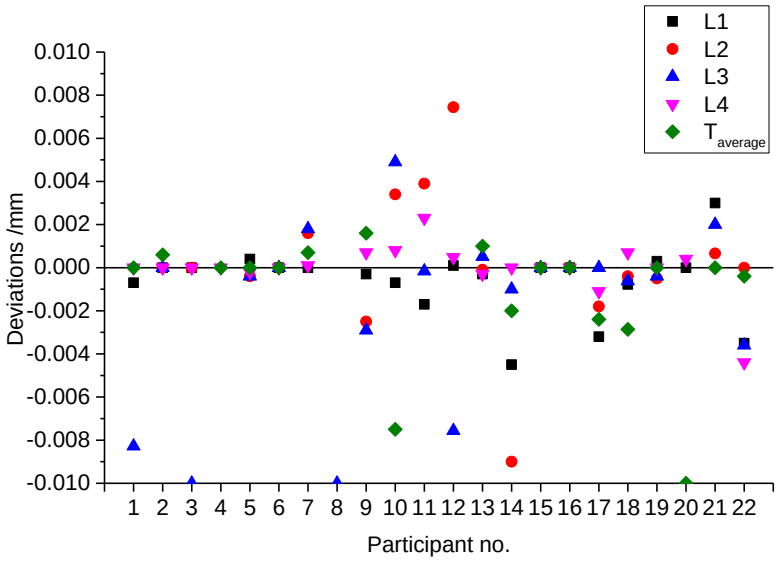

(c)

Figure 17. Deviations between two scanning approaches for all measurands: (a) deviation range ± 0.08 mm, (b) deviation range ± 0.04 mm, and (c) deviation range ± 0.01 mm

4.5. Agreement between participants and reference measurements

In order to ensure the agreement between reference measurements and participant measurements, the E_n value normalised with respect to the stated uncertainty was used according to ISO guidelines [ISO/IEC 17043, 2010]. The E_n value is defined as follows

$$E_n = \frac{x_{part} - x_{ref}}{\sqrt{U_{part}^2 + U_{ref}^2}}. \quad (2)$$

Here, x_{part} is the measurement obtained by the participant and x_{ref} the reference value, while U_{par} and U_{ref} are the corresponding expanded uncertainties. If $|E_n| < 1$, there is agreement between the reference measurement results and the participant results. This is not the case if $|E_n| \geq 1$. **Figure 18**, **Figure 19**, **Figure 20**, **Figure 21**, **Figure 22** show the distribution of E_n values calculated for Assembly 1.

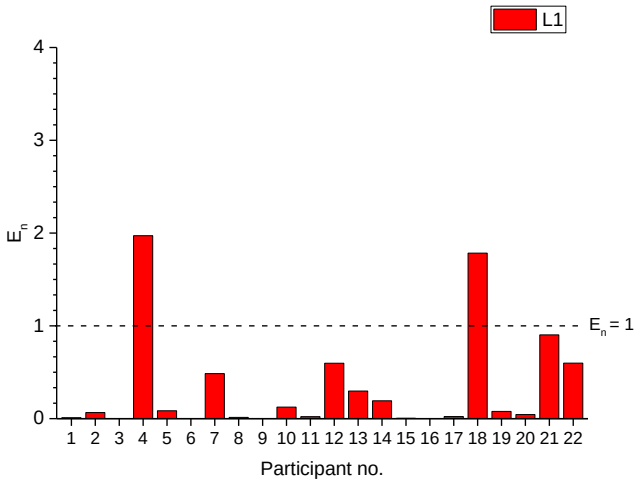

(a)

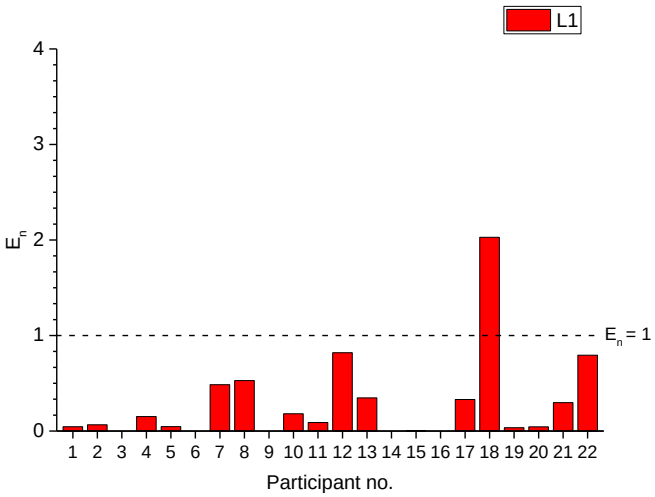

(b)

Figure 18. E_n values for the measurements of L1: (a) Own Choice approach (b) Fast Scan approach

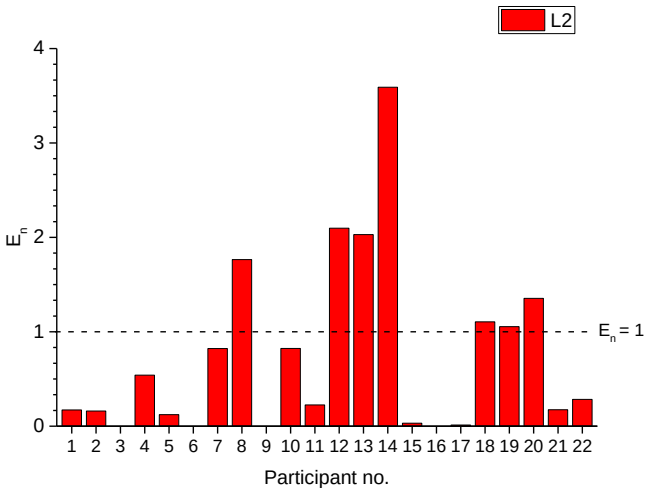

(a)

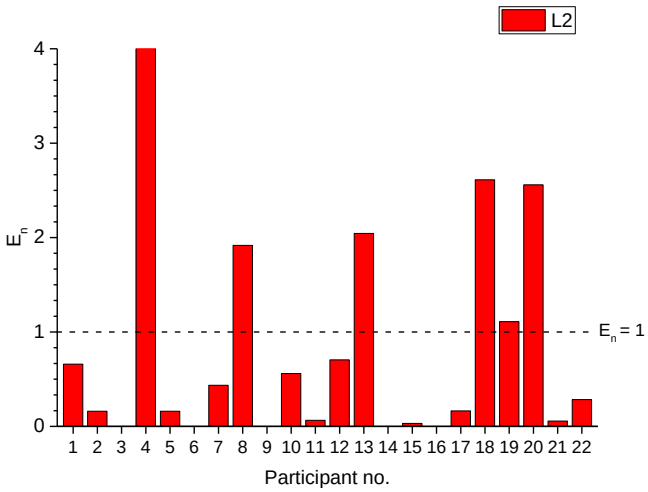

(b)

Figure 19. E_n values for the measurements of L2: (a) Own Choice approach (b) Fast Scan approach

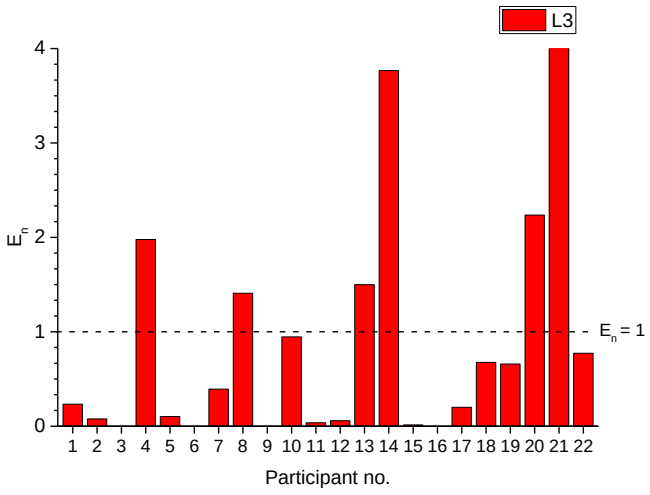

(a)

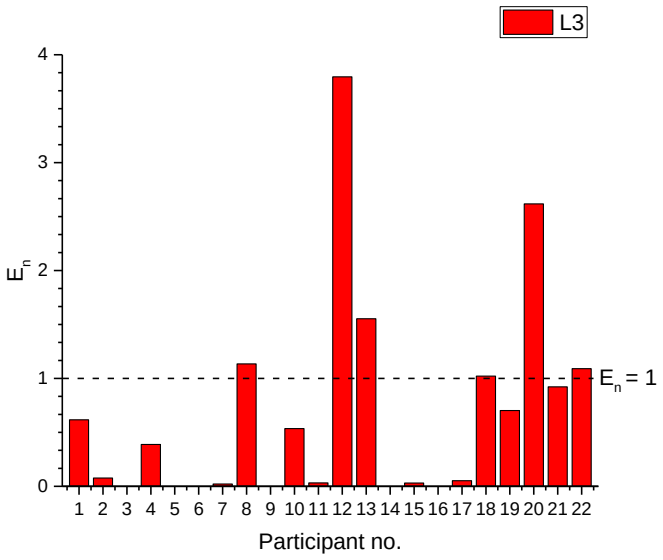

(b)

Figure 20. E_n values for the measurements of L3: (a) Own Choice approach (b) Fast Scan approach

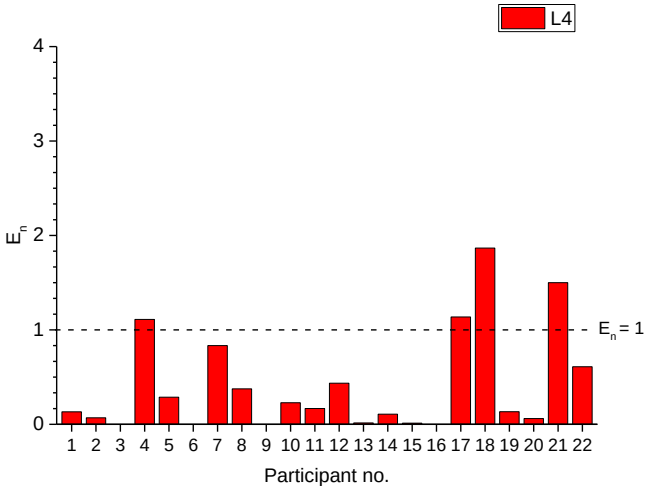

(a)

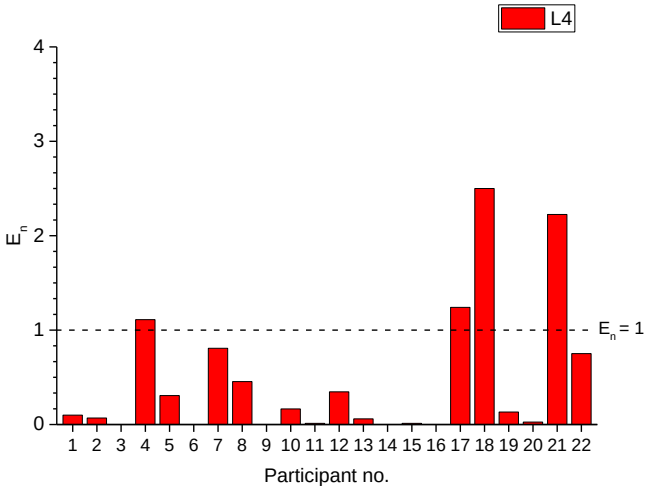

(b)

Figure 21. E_n values for the measurements of L4: (a) Own Choice approach (b) Fast Scan approach

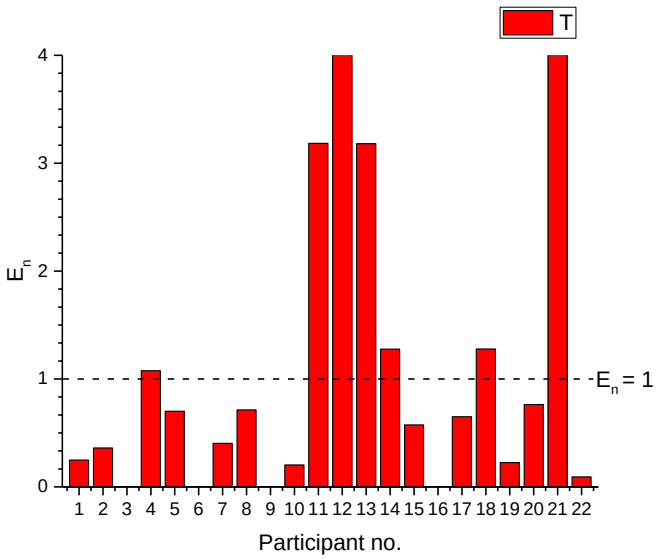

(a)

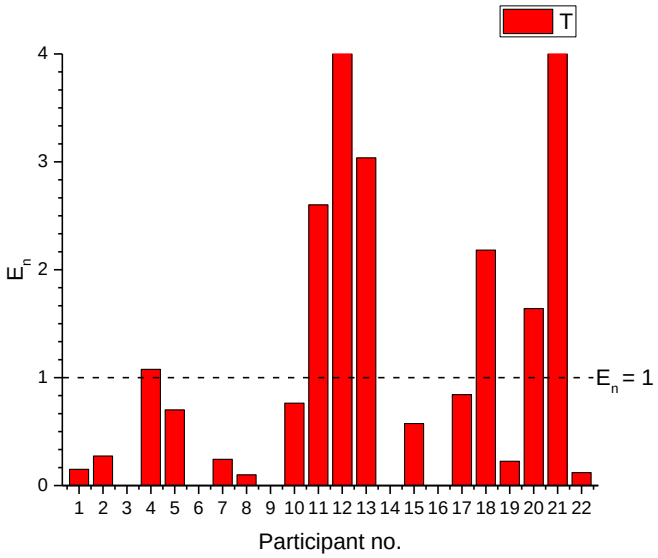

(b)

Figure 22. E_n values for the measurements of $T_{average}$: (a) Own Choice approach (b) Fast Scan approach

71% of the measurements conducted using the Own Choice approach are in agreement with the reference values. 59% of the measurement results carried out using the Fast Scan approach are in accordance with the reference values. The E_n values of measurements based on Fast scan choice approach are up to 35% bigger than those ones obtained using the Own choice approach. The level of agreement strongly depends on the measurands. *L2* and *L3*, which are

bidirectional measurands, show lower agreement than *L1* and *L4*, which are unidirectional lengths. The latter normally raise no problems due to their high robustness against noise and beam hardening artefacts. *T* shows worse agreement than L3 despite their similarities (both are bi-directional length of similar size). This result confirms the higher difficulty in defining a multi-material surface determination and a stable datum system for measurements of *T* compared to *L3*. The larger deviations registered for *T* may also be explained by the position of the measurand within the measured volume. *T* does not lie in the centre of the beam as *L3* does, which may result in incrementing reconstruction errors leading to inaccurate measurement results.

Measurements of *L2* are smaller than the calibration values, whereas *L3* are generally larger. This difference is due to the impact of noise and beam hardening on the surface determination and measurements. *L1* and *L4* present similar deviations despite the different size.

Figure 23 shows that participants all present trend of measurement deviations despite having different amplitudes. The trends of measurement deviations provide evidences that most of X-ray systems suffer from geometrical errors. The different amplitudes of measurement deviations indicate that some participants were able to minimise systematic errors while others were not. The participants who efficiently corrected systematic errors showed deviation in the order of surface texture of Assembly 1 (Ra = 0.40 ± 0.05 µm and Rz = 2.20 ±0.05 µm).

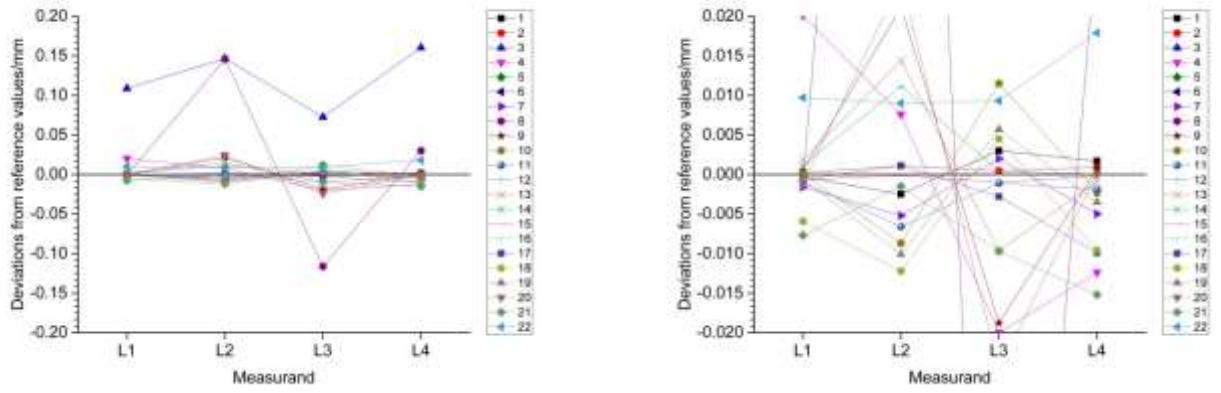

(a) (b)

Figure 23. Trends of deviations for the four measurands, L1, L2, L3, and L4: (a) deviation range ± 0.20 mm and (b) deviation range ± 0.020 mm

Figure 24 and **Figure 25** show the deviations of *L1*, *L2*, *L3*, *L4*, and *T* for the two scanning approaches. By using the scatter plots, it can be observed that *L1* shows that all participants are close to one another, whereas the remaining measurands show larger differences among the

participants. The number of measurement outliers does not increase among the measurands, whereas the distribution spread does. Narrower distributions can be seen for *L1* and *L4* with respect to *L2*, *L3*, and T. The distributions of measurements of L1 and L4 present similar standard deviations values, suggesting that repeatability of inspections does not change as the size of a measurand increases. The spread of distributions can be used for highlighting the impact of noise on the measurement results.

None of the distributions of deviations has zero mean, proving the presence of systematic errors. The spread of distributions varies with the scanning approaches. The Own Choice approach resulted in smaller distributions compared to the Fast Scan approach.

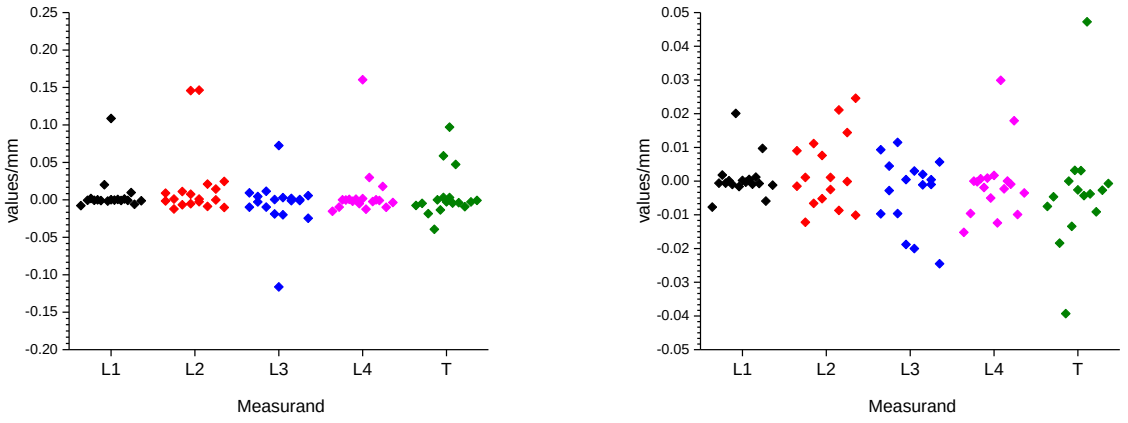

Figure 24. Scatter plots for the four measurands, L1, L2, L3, and L4, scanned using the Own Choice approach: (a) deviation range ± 0.25 mm and (b) deviation range ± 0.05 mm

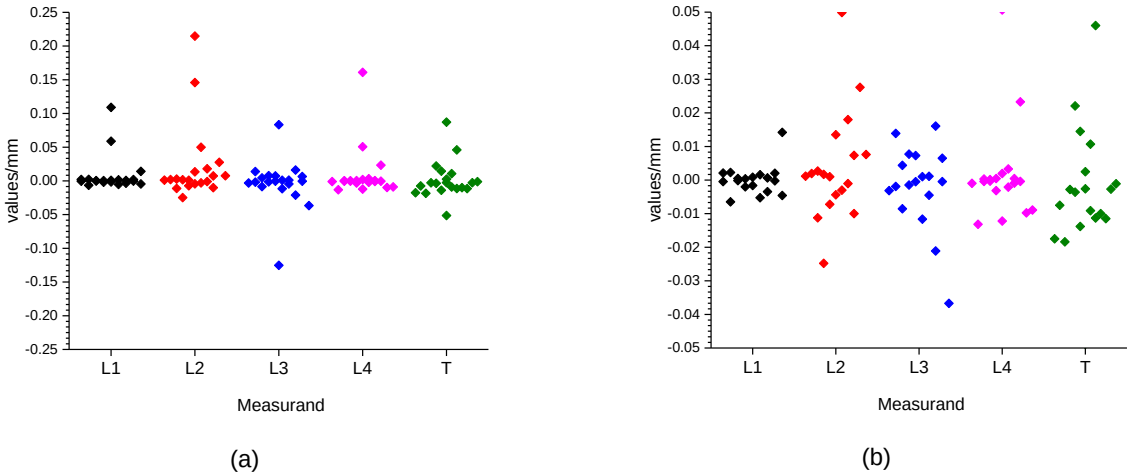

Figure 25. Scatter plots for the four measurands, L1, L2, L3, and L4, scanned using the Fast Scan approach (a) deviation range ± 0.25 mm and (b) deviation range ± 0.05 mm

4.6. Industrial CT scanners used by the participants

The frequency of industrial CT scanners used is shown in **Figure 26.** Most of participants have access to CT systems for dimensional measurement while a very small number of participants possess CT systems for general applications. Two main constructive differences between CT for dimensional measurement and CT for general applications are in the accuracy of the positioning system (resolution ≤ 0.2 µm) and in the stability of the cabinet temperature throughout the course of the inspection time. The frequency of MPE values is shown in **Figure 27**. The MPE is defined as the extreme value of the error of indication of a CT for a given size measurement *L*. The majority of manufacturers declare a MPE value of 9 ± L/50.

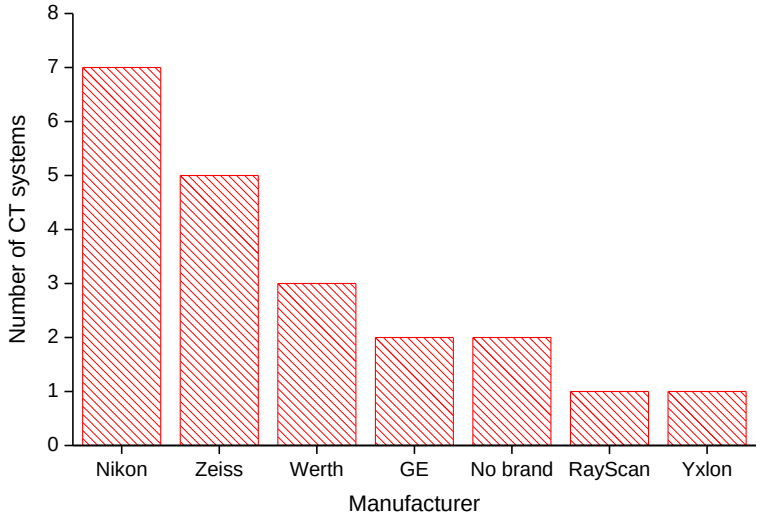

Figure 26. Brands of CT systems used within this comparison

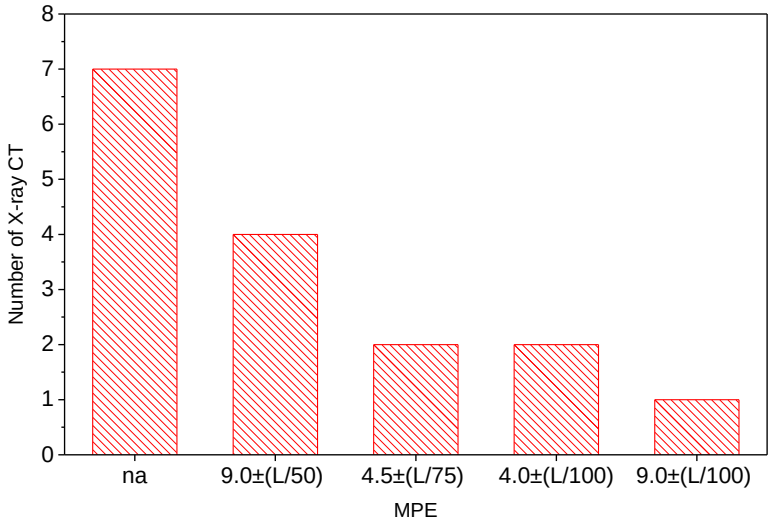

Figure 27. Frequency of MPE values

4.7. Software adopted by the participants

6 out of 18 participants used acquisition and reconstruction software developed by Nikon, see **Figure 28** and **Figure 29**. 14 out of 18 participants had analysis software of the type VGStudioMAX, see **Figure 30**. Moreover, two participants used in-house software for image acquisition.

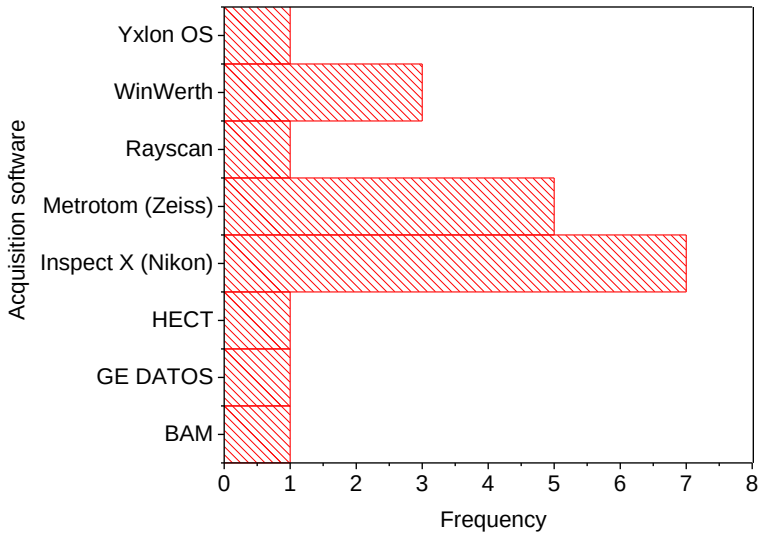

Figure 28. Frequency of acquisition software used within this comparison

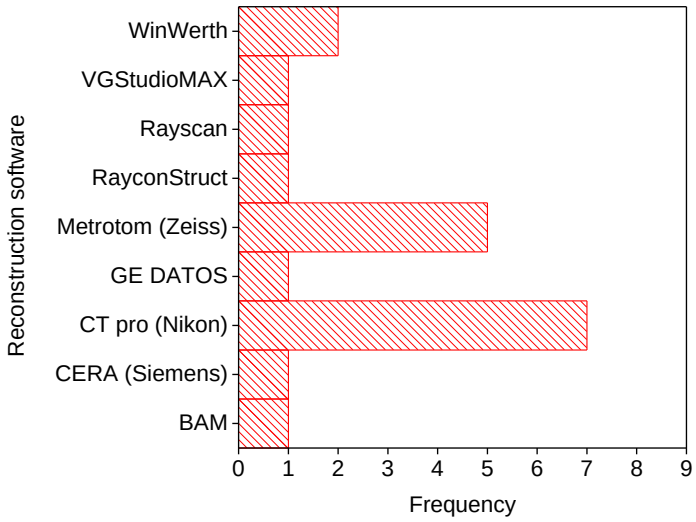

Figure 29. Reconstruction software used in this comparison

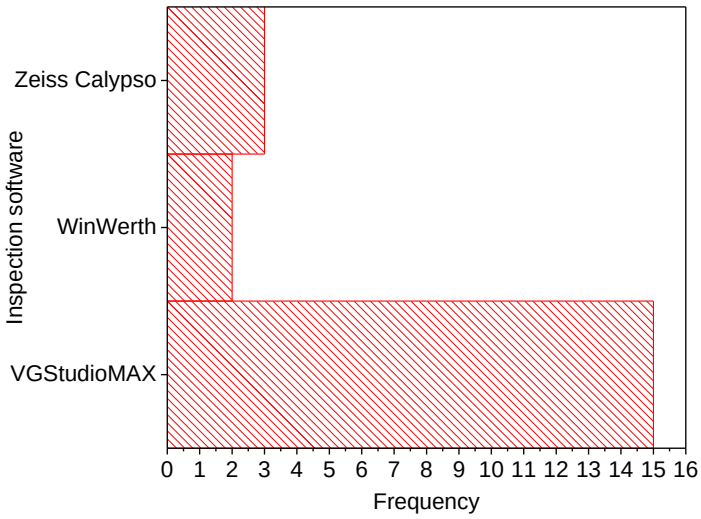

Figure 30. Analysis software adopted within this comparison

4.8. Assembly 1: Impact of instrument settings and operator

18 out of 22 participants orientated the samples in an inclined way (see **Figure 31**) in order to decrease the beam angle, which directly influences the Feldkamp artefacts. 14 out of 22 participants applied a physical filter on the gun to re-shape the X-ray spectrum towards high energy, see **Figure 32** and **Figure 33.** 10 of the 14 participants used cupper (*Cu*), 2 out of 22 participants used tin (*Sn*), 1 out of 14 used iron (*Fe*), and 1 of the 14 used aluminium (*Al*). *Cu* has a higher photoelectric absorption than Compton scatter which makes it an efficient filter for industrial applications. The photoelectric coefficient varies with energy and atomic number. The Compton coefficient is independent of energy and almost independent of atomic number. The K-shell binding energy of *Cu* is 9 keV, resulting in absorbing X-rays in the range of 9 - 30 keV. *Sn* has a K-shell binding energy of 29.2 keV, leading to absorbing photons of energies in the range of 30 - 70 keV through photoelectric interactions. This includes the characteristic radiation produced by X-ray target materials (e.g.tungsten or copper). 1 out 20 participants used *Sn* together with Cu in order to compensate for the characteristic radiation generated by *Sn*. The K-shell binding energy of *Fe* resembles the one of *Cu*. The K-edge of *Al* is 1.56 keV, resulting in only absorbing low energy X-rays. *Al* can be used as filters for very soft materials, such as polymers, or for absorbing the X-ray fluorescence coming from filter with higher atomic number. X-ray fluorescence (XRF) is the emission of secondary X-rays from a material that has been excited by high-energy X-rays.

12 out of 22 participants scanned Assembly in good thermal conditions (T = 20 ± 1 °C), while the remaining participants conducted their investigations in environments above 22 °C. An overview of the temperature during scanning is given in **Figure 34**. No information regarding the exact measuring points of the temperature is available. Apart from the impact on the dimensional stability of samples and manipulator system, higher temperatures degrade the detector efficiency (DQE) and increase the dark current leading to noise.

12 out of 22 participants scanned Assembly 1 one time, (see **Figure 35**), 8 out of 22 participants had scanned Assembly 1 more than. A few participants repositioned the samples between two subsequent scans. Participant no. *12* scanned the sample 10 times using the Fast Scan procedure. This approach did not meet the technical protocol.

7 out of 22 participants performed a scale error correction using a reference artefact, as shown in **Figure 36**. Sphere-to-sphere distances or hole-to-hole distances were used for the correction. The correction of scale was conducted on both CT equipped with and without laser corrected

linear guideways. The reference artefacts were also used for quantifying the measurement uncertainties. Other hardware corrections conducted by participants included detector calibration, which corrects for the non-uniform response of detector pixels, and axis qualification. Ring artefact corrections were conducted before scanning. Ring artefact corrections were based on either swimming of the workpiece across the detector by a few detector pixels or by post-processing the acquired projections.

The values of the current and voltage used for imaging the samples are shown in **Figure 37** and **Figure 38**. It can be seen that higher voltage and current values were used for the Fast-scan-based measurements compared to the Own-choice-based measurements. An average voltage of 169 kV and of 173 was used for Own-choice-based measurements and Fast-scan-based measurements, respectively. As a result, the power varied between the two scanning approaches, as shown in **Figure 39**. Higher power levels leads to increasing X-ray focal spot size and reducing the structural resolution. No statistical correlation was identified between the measurement accuracy and the used voltage. It is believed that the voltage and current levels has an impact until the sample is fully penetrated at any angular positions. Once the complete penetration of a sample is reached, further increases in voltage and current do not gain any sizeable improvements in the accuracy of measurement results.

Voxel sizes used by the participants are reported in **Figure 40** and calculated based on the detector pixel size *p*, the source-detector distance *SDD* and the source-object distance *SOD*. The deviations from reference values with respect to the voxel size are given in **Figure 41** for both scanning approaches. No statistical correlation was found between the measurement accuracy and the voxel size in this work. It is believed that voxel size has no impact on the accuracy of a feature whose size is far larger than the voxel one.

The prevalence of integration time is shown in **Figure 42**. The integration time strongly depends on the detector and on the power used. Longer integration times reduce the image quality due to dark current.

Most of participants used image averaging to improve the image quality as depicted in Figure 43. One image per projection was the most selected value. A few participants set 4 or even more frames per projection. It should be reported that Participants no. *1*, *2*, *9*, and *15* chose more than one image per projection for scans conducted using the Fast Scan procedure.

Image averaging and integration time can synergically be used for improving image quality and reducing scanning time. For example, an integration time of 1 s and an image averaging of

four frames produce the same image quality as an integration time of 4 s and no image averaging. However, the scanning time is shorter.

Frequency of binning strategy is shown in **Figure 44.** Binning improves the image quality by merging groups of pixels, typically 4, into virtual pixels. The major limitation of binning is that it reduces the structural resolution.

The frequency of scanning time is shown in **Figure 45**. An average scanning time of 191 min was registered for Own-choice-based measurements, with a maximum scanning time of 1120 min. An average scanning time of 40 min was used for Fast-scan-based measurement, with a minimum scanning time of 9 min. Measurement deviations with respect to the scanning time are showed in **Figure 46**. It can be seen that even short scanning times lead to measurements with micrometre accuracy.

Most of participants used an advanced thresholding method for segmenting the CT data sets. The surface determination was based on the average grey value intensity of the background and of the aluminium step gauge. Three participants used the region growing method starting from a seed point selected within the aluminium region of Assembly 1. Two further participants used a Werth method whose features are not disclosed.

The frequency of backprojection filtering is shown in **Figure 47**. Ramp filters, Shepp-Logan filters, and Henning filters are types of filters adopted within this comparison. Ramp filters are a kind of back-projection filter having no cut-off at high frequencies. Sheep-Logan and Henning filters present cut-offs at high frequencies. Sheep-Logan filters have less impact on the structural resolution compared to Hanning filters.

5 out of 18 participants applied a software beam hardening correction while reconstructing. 3 of those participants, who applied software beam hardening correction, did not apply physical filter on the X-ray tube. None of participants applied volume filtering, such as mean, median or Gaussian filters, as they yield a negligible performance advantage in dimensional measurements.

Frequency of voxel (volume) and STL (surface) data is shown in **Figure 48**. No information regarding the number of triangles used for creating STL data sets was provided.

Investigations were all conducted in accordance with the technical protocol in terms of datum system and feature evaluations. Elementary feature such as cylinders, planes and lines were used for defining the datum system and the five measurands. Most participants did not use the CAD model provided for alignment or evaluation. Some participants used the CAD model

provided to set the measuring strategy. The CAD model was subsequently aligned with the voxel model using a best fit method and all features were moved from it to the voxel model.

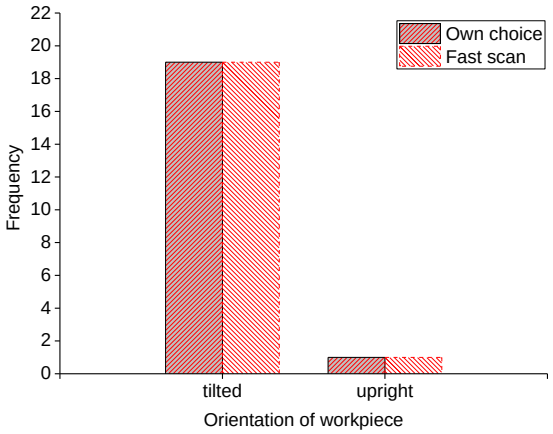

Figure 31. Orientation of Assembly 1

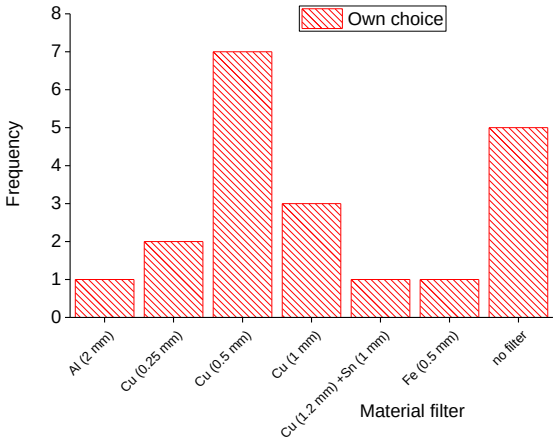

6

Figure 32. Pre-filter material and thickness in mm for Assembly 1 (Fast Scan approach)

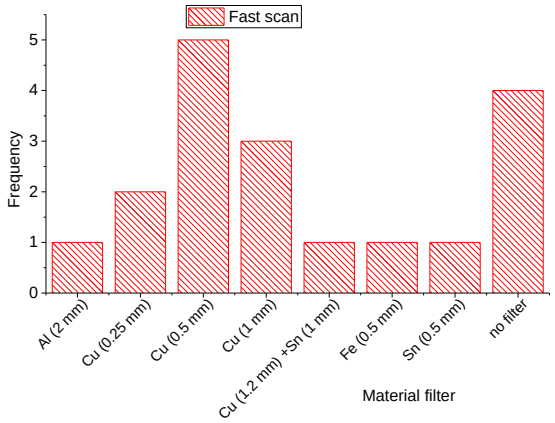

Figure 33. Pre-filter material and thickness in mm for Assembly 1 (Own Scan approach)

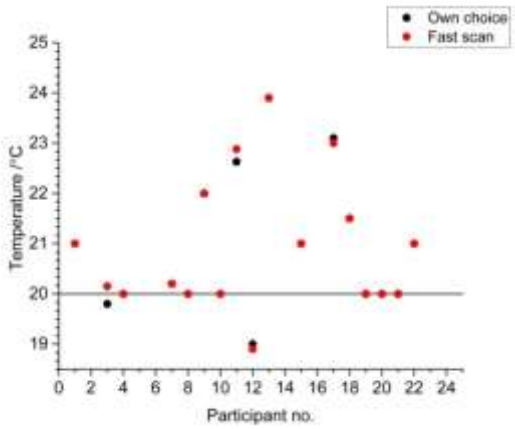

Figure 34. Temperature inside the CT scanner

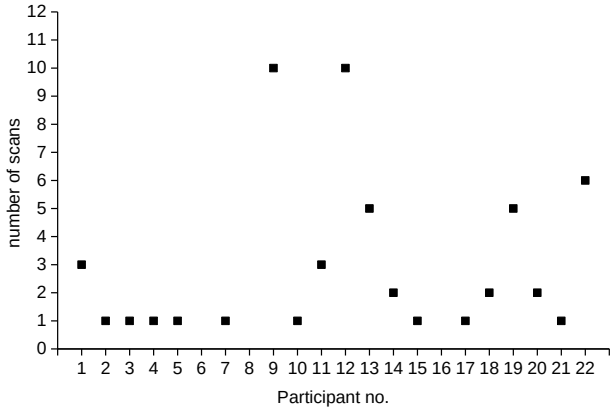

Figure 35. Number of scans per participant

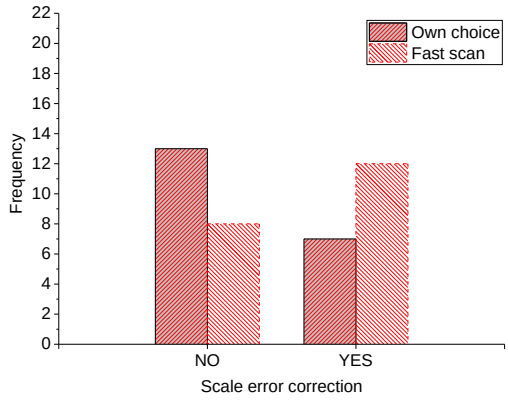

Figure 36. Scale error correction

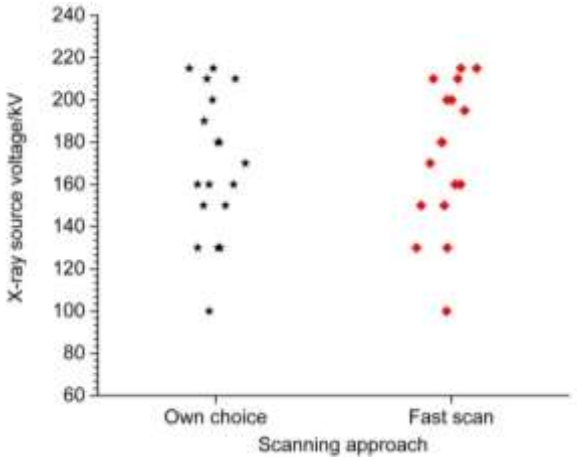

Figure 37. X-ray source voltage for both scanning approaches

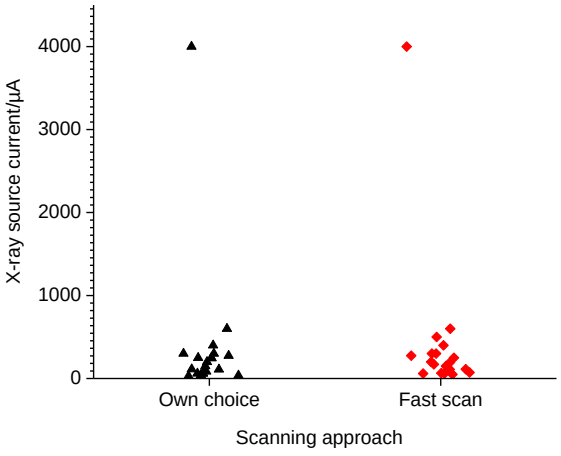

(a)

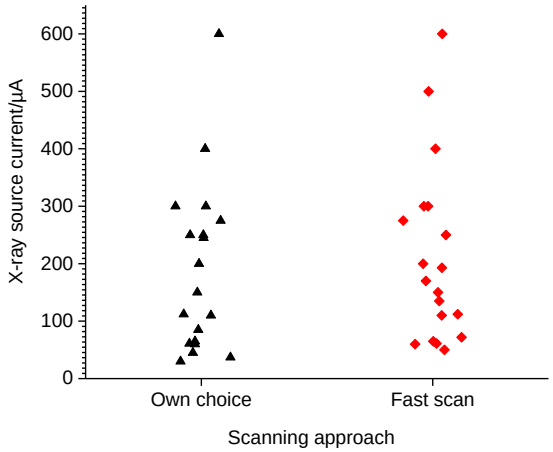

(b)

Figure 38. X-ray source voltage for both scanning approaches: (a) range up to 4500 µA and (b) range up to 600 µA.

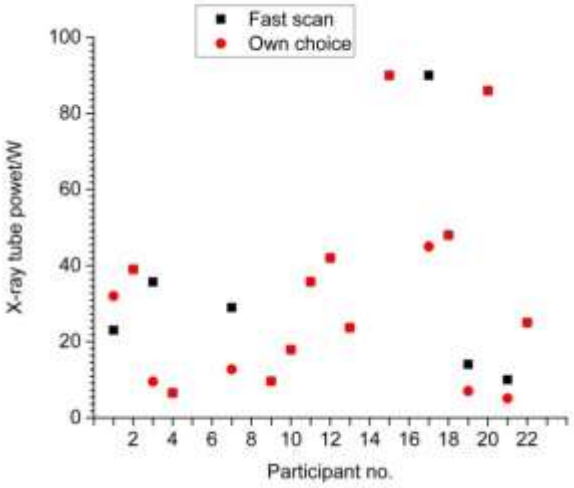

Figure 39. Power used for both scanning approaches, range up to 100 W.

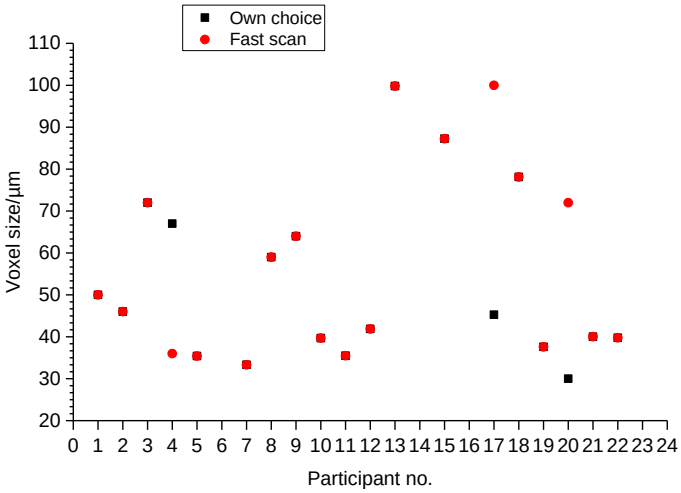

Figure 40. Voxel sizes used for both scanning approaches

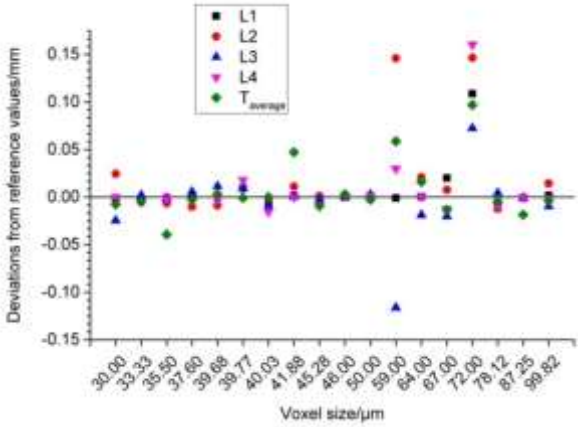

(a)

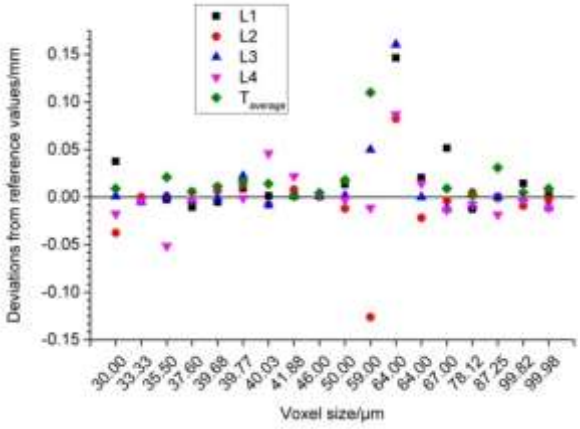

(b)

Figure 41. Deviation from reference values vs. voxel size for Item Assembly 1: (a) Own Choice approach, and (b) Fast Scan approach.

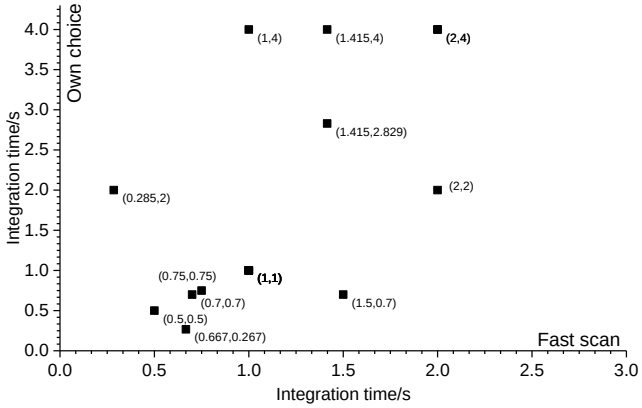

Figure 42. Frequency of integration time

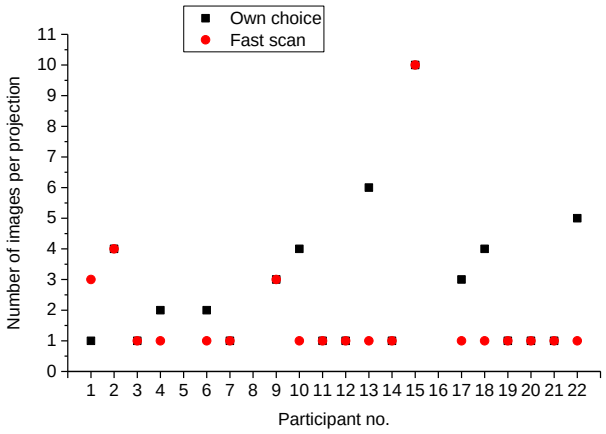

Figure 43. Number of image averaging for both scanning approaches

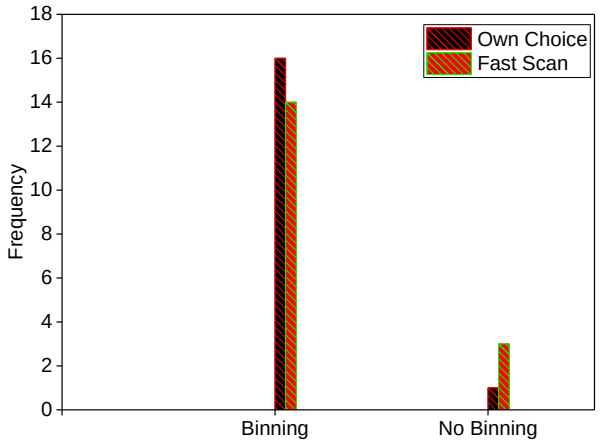

Figure 44. Binning mode used for both scanning approaches

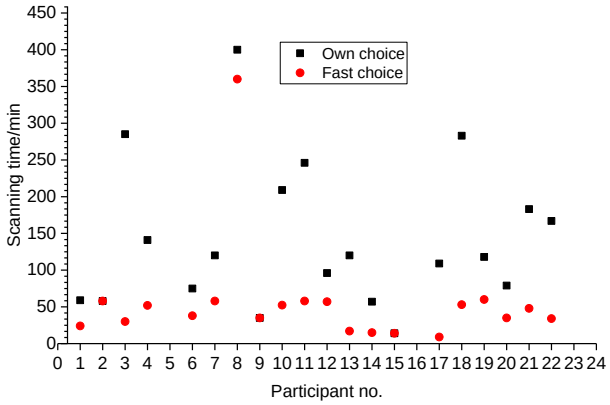

Figure 45. Scanning time for both scanning approaches

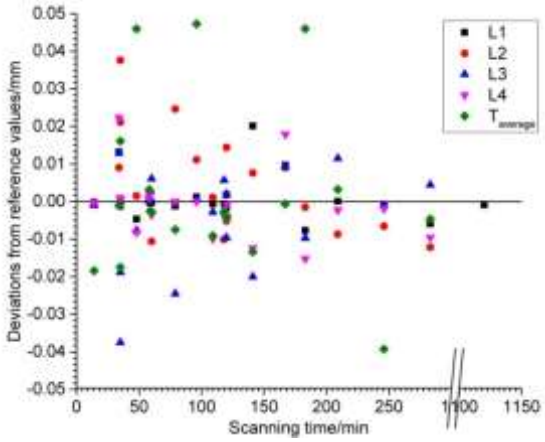

(a)

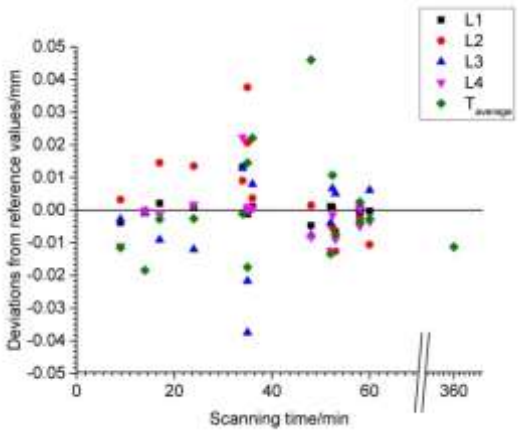

(b)

Figure 46. Deviation from reference values vs. scanning time for Assembly 1: (a) Own Choice and (b) Fast Scan. Range ± 0.05 mm

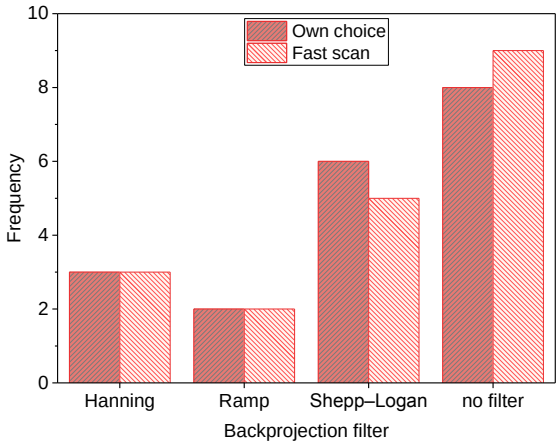

Figure 47. Backprojection filters used for both scanning approaches

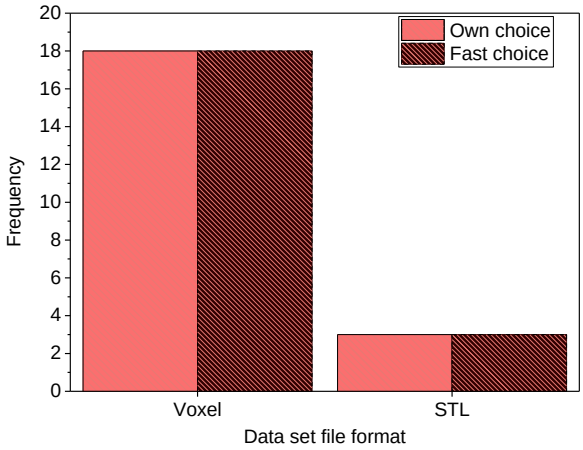

Figure 48. Data set file types for both scanning approaches

4.9. Assembly 1: measurement uncertainties provided by the participants

The uncertainty methods applied by the participants are shown in **Figure 49**. 5 of the 22 participants used the MPE. 6 out of 22 participants used more complex measurement uncertainty approaches which relied on reference objects scanned before or after the sample of Assembly 1. The environment temperature, the system repeatability, voxel size, probing error, detector errors, and rotary table errors represent the further considered contributions. Finally, 3 of the 22 participants did not provide any measurement uncertainty statement. The frequency of uncertainty izes for Assembly 1 is shown in **Figure 50** and in **Figure 51** for measurements conducted using the Own Choice approach and the Fast Scan approach, respectively. The presented uncertainty values comprise all the uncertainty provided by participants. Two main observations can be drawn from the figures. First, the measurement uncertainties can be clustered in 5 groups having increasing magnitudes. The majority of participants stated values below 10 µm (≈ MPE) for all measurands. 2 out of 20 participants stated measurement uncertainties above 30 µm. The second observation is that larger measurement uncertainties were stated for Fast Scan´s measurements than for Own Choice´s ones. The increase of measurement uncertainties is mainly observed for the bi-directional measurements, which are more sensitive to surface noise.

As just mentioned, Most of the participants identified in the MPE value of their own CT systems an estimation of measurement uncertainty. Despite its simplicity, the use of MPE presents three potential limitations. First, the MPE is quantified from scanning conditions which may not totally reflect the scans produced for the comparison. For example, the reference object used for quantifying the MPE may be different from Assembly 1 in terms of size, material and measurands. Second, the MPE is based on centre-to-centre distances which are representative of uni-directional measurands, L1 and L4, but not of bi-directional measurands, L2, L3, and T. Third, the MPE, being defined as a range, needs to be converted into an uncertainty contribution using e.g. one of the probability distributions listed in the GUM. Most did not apply any distribution for converting the MPE into an uncertainty contribution. As a consequence, the MPE does not fully meet the requirement of similarity between features that is necessary for establishing traceability in this comparison.

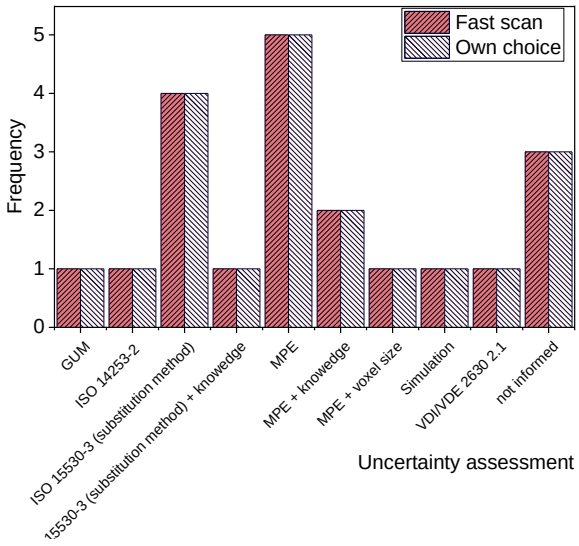

Figure 49. Frequency of applied uncertainties by the participants

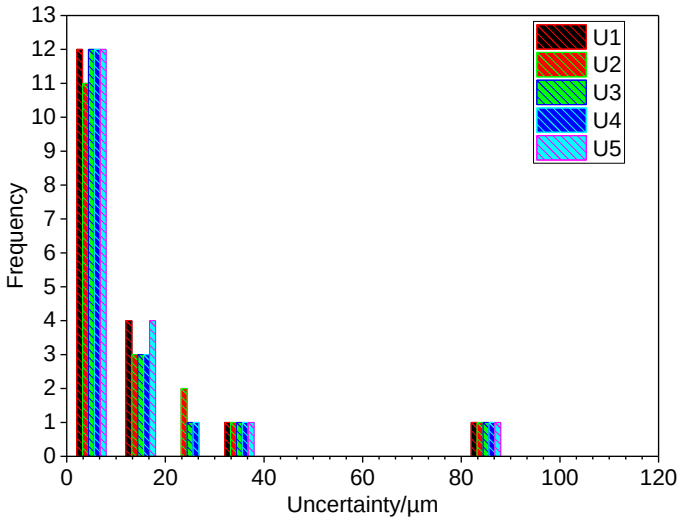

Figure 50. Histogram of uncertainty sizes for Assembly 1 scanned using the Own Choice approach

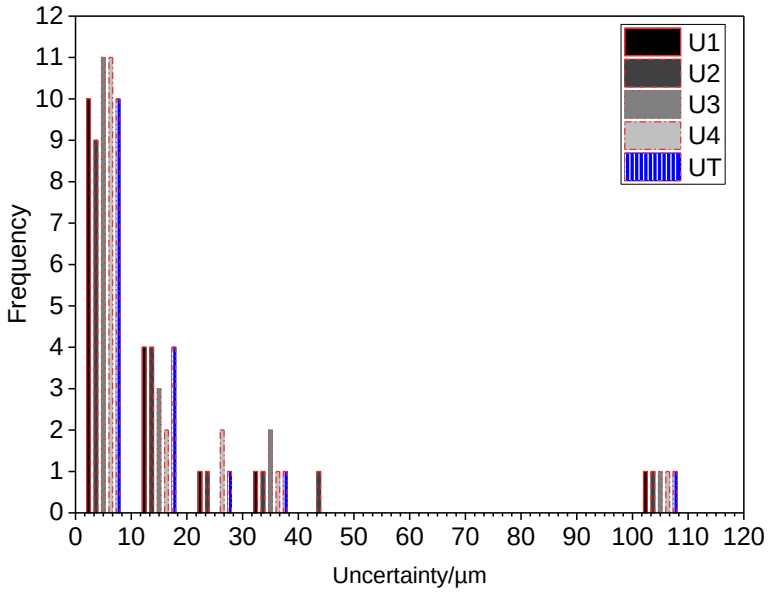

Figure 51. Histogram of uncertainty sizes for Assembly 1 scanned using the Fast Scan approach

4.10. Main results for Assembly 2

13 participants measured Assembly 2. Their results are shown in Figure 51 for the inspections conducted on the *HR* data sets and in Figure 52 for the inspections on the *LR* data sets.

Figure 51 shows that there is a very good agreement among most participants' results for *D1* and *D2*, with a range of variation of approximately 2 µm. 2 out of 13 participants provided measurement result of *D1* and *D2* which is slightly different from the others. Figure 51 evidences that there is still a good agreement among participants in connection with *R1* despite a larger variation among participants of approximately 9 µm. The variation in the results can be due to different approaches for surface determination and different software used for the inspections. Ultimately, Figure 51 depicts the results for *C1* highlighting a worse agreement amid participants. The range of variation of measurements is of approximately 68 µm. Concentricity is well known to be one of the most difficult tolerances to measure due to its difficulty in establishing the mid points of the feature. Therefore, the large variability can be due to errors in establishing a robust alignment system for quantifying concentricity.

Figure 52 displays that there is a very good agreement among most participants' results for *D1* and *D2* of the *LR* data sets. The range variation does not change with respect to the HR data sets. 1 of the 13 participants provided measurement result for *D2* that is slightly different from the others. Wider variation among participants is observed in connection with *R1*, with a range of variation of measurements is of approximately 14 µm. The range of variation increases by more than 10% compared to the same measurements conducted on the HR data sets. The increase in the variability may be due to the fact that increasing the surface noise would magnify the differences among surface determination approaches. The figure shows that the range of variation for *C1* increased by just 5% for the *LR* data sets compared to the same measurements conducted on the *HR* data sets.

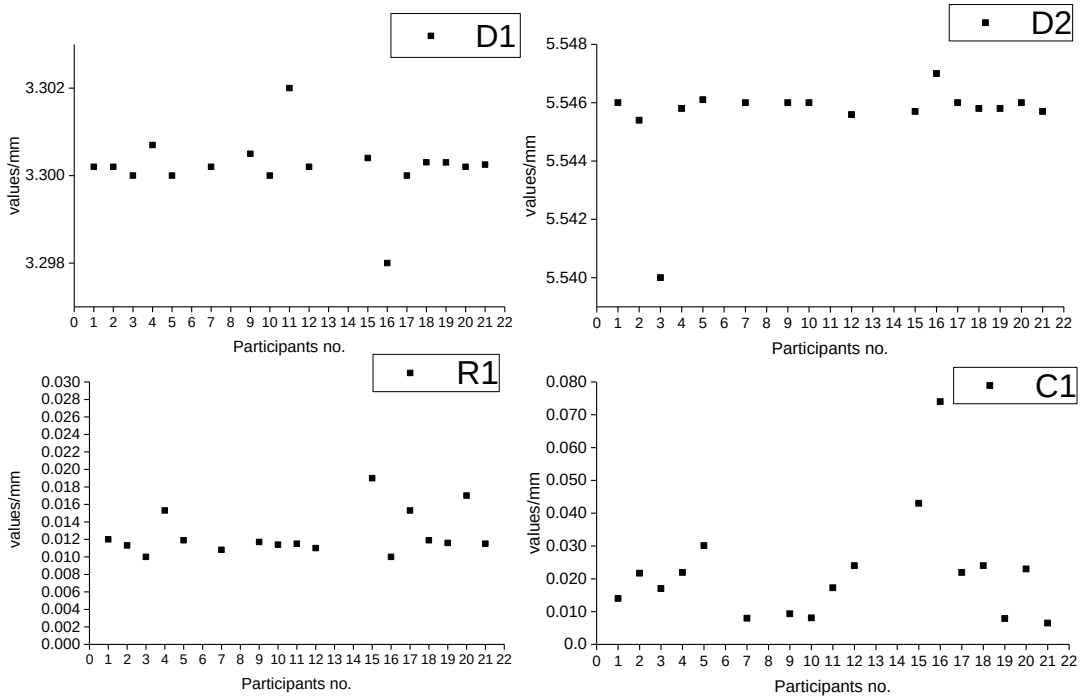

Figure 52. Results for Assembly 2 (HR data sets)

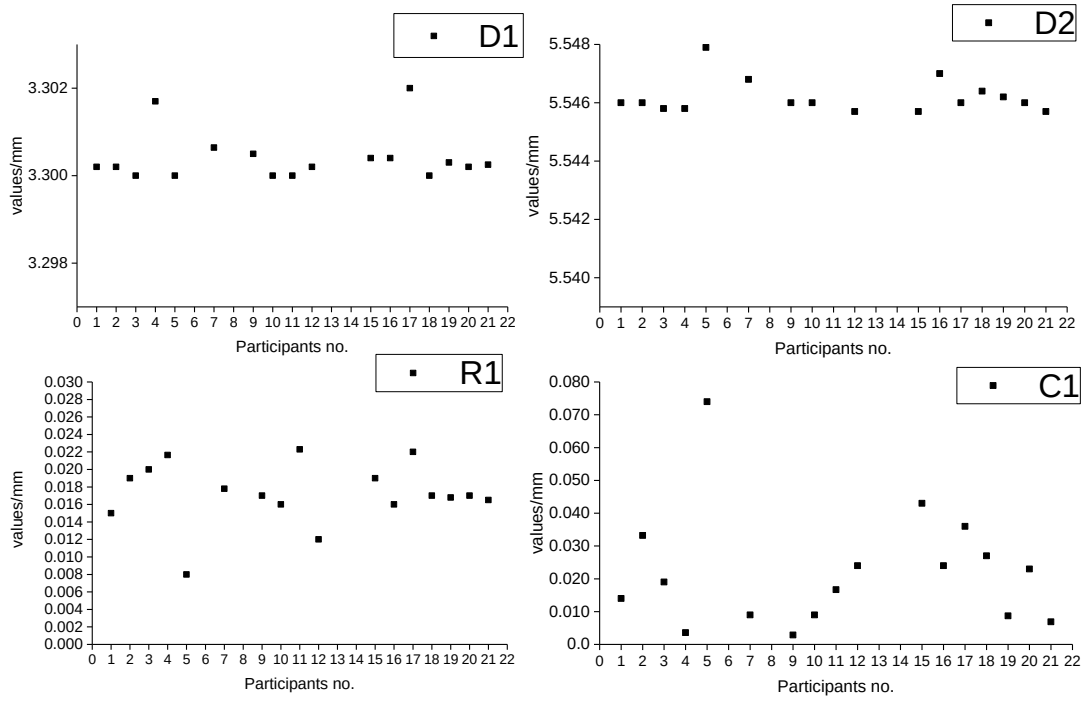

Figure 53. Results for Assembly 2 (LR data sets)

4.11. Assembly 2: Impact of Operator

Regarding the inspection software, 16 out of 17 participants used VGStudioMAX inspection software, while only one participant used Zeiss Calypso. Different versions of VGStudioMAX were used by the participants, which may to some extent explain differences among the participants. Surface determination was based on advanced methods that all take into account the local behaviour of the grey values. Some participants applied morphological operators, such as opening and closing, before segmenting the data sets. Opening removes small objects from the foreground (usually taken as the dark pixels) of an image, placing them in the background, while closing removes small holes in the foreground, changing small areas of background into foreground. A typical use of opening and closing is for removing noise.

None of the participants filtered the volume using volumetric filters to minimize the effect of noise and of surface texture on R1.

The frequency of voxel (volume) and STL (surface) data is shown in Figure 48. Although the data sets were distributed as voxel files, some participants decided to work on STL files. No substantial difference between measurements conducted using voxel files and STL files were observed due to the almost totally absence of image artefacts within the data sets. STL files reduced the amount of data being handled by more than 90%. The majority of investigations were conducted in accordance with the technical protocol provided by the coordinator. Minor changes were however registered between the participants´ measuring strategies and the technical protocol. The most recurring difference was the change of size of primary datum, a cylinder, in order to cope with the taper of Assembly 2. Elementary feature such as cylinders, planes, and circles were used for defining the datum system and the five measurands. Most of participants used the CAD model for alignment and evaluations. Some participants used the CAD model for more easily setting the measuring strategies. The CAD model was subsequently aligned with the voxel model using a best fit method and all features were moved from it to the voxel model.

Evaluations of the features were conducted in different ways especially for the concentricity. The majority of participants measured concentricity using the software script, while some others quantified the concentricity measuring the maximum distance between the median point of the cross section and the reference datum.

5. Conclusions

The conclusions of this comparison are summarized as follows:

- Circulation started in January 2016 and was completed in August 2016. 22 participants from 7 countries have participated.
- Thanks to excellent support by all participants, the circulation followed the initial schedule, except for three participants who were delayed due to scanner problems.
- 22 samples of Assembly 1 were manufactured, measured at CGM and circulated in parallel.
- 1 samples of Assembly 2 was selected from industrial production, scanned and electronically distributed to all participants at two levels of image quality (HR and LR).
- Different measurands were considered, encompassing lengths, diameters, roundness, concentricity. A multi-material length was also considered.
- Two different scanning approaches were considered for Assembly 1. The first approach, coded as “Own Choice”, does not apply any scanning restrictions on any of the scanning parameters. The second one, coded as “Fast Scan”, introduced a series of limitations, including the scanning time and the number of images per projection.
- One single inspection procedure was defined for Assembly 2.
- Reference values for all samples of Assembly 1 and Assembly 2 were provided using a coordinate measuring machine.
- Depending on the item and measurand, the reference expanded uncertainties (k=2) ranged from 1.1 µm to 2.6 µm.
- The stability of Assembly 1 was documented throughout the course of the comparison.
- All samples of Assembly 1 have shown a good stability through the approximately 8 months circulation.
- The measuring procedures were followed by all participants without problems.
- Results by the single participants were compared with the reference values provided by CGM.
- Each participant can use the comparison results to verify the performance of CT system and to compare own measurement strategies and measurement uncertainties.
- The majority of participants stated measurement uncertainties below 10 µm for all measurands of Assembly 1.

- 71% of the measurements for Assembly 1 conducted using the Own Choice approach are yielded $|E_n| < 1$, while 59% of the measurements based the Fast Scan approach yielded $|E_n| < 1$.
- The majority participants obtained similar results in both scanning approaches. A few participants achieved significantly different measurement results, most probably due to the impossibility of selecting suitable scanning parameters.
- *L2* and *L3*, which are bidirectional measurands, show lower agreement than *L1* and *L4*, which are unidirectional lengths.
- *T* shows worse agreement than *L3* despite their similarities (both are bi-directional length of similar size). This result confirms the higher difficulty in defining a multi-material surface determination.
- A very good agreement was seen among most participants' results for *D1* and *D2* from Assembly 2. The range of variation was approximately 2 µm
- A good agreement was also seen among participants in connection with *R1 of* Assembly 2, with a range of variation of measurements of approximately 9 µm and of 11 µm for *HR* and *LR* data sets, respectively.
- A worse accordance was registered for *C1 of* Assembly 2, with a range of variation of measurements of approximately 68 µm and of 72 µm for *HR* and *LR* data sets, respectively.
- 12 of the 22 participants had scanned Assembly 1 in good thermal conditions (20 ±1 °C), while the remaining participants conducted their investigations in environments above 22 °C.
- 2 of the 22 participants scanned Assembly 1 once, 8 out of 22 participants had scanned Assembly 1 more than once as so. A few participants repositioned the samples between two subsequent scans.
- 7 out of 22 participants performed a scale error correction before scanning samples.
- Detector calibration, axis qualification and ring artefact corrections were the other types of corrections applied by participants.
- 14 out of 22 participants applied a physical filter on the gun to re-shape the X-ray spectrum towards high energy. 0.5-mm-Copper was the most used physical filter.
- Higher voltage and current values were used for the Fast-scan-based measurements compared to the Own-choice-based measurements. An average voltage of 169kV was

used for the Own-Choice-based measurements, while an average voltage of 173kV was used for Fast-Scan-based measurements, respectively.

- Most of participants selected more than one image per projection, a few of whom used 4 or more frames per projection.
- An average scanning time of 191 min was registered for Own-choice-based measurements, with a minimum scanning time of 14 min. An average scanning time of 40 min was used for Fast-scan-based measurement, with a minimum scanning time of 9 min.
- 17 participants stated a measurement uncertainty per measurand, with MPE as the most common estimator.
- 6 out of 22 participants used more complex measurement uncertainty approaches including influence factors such as temperature, the system repeatability, voxel size, probing error, detector errors, and rotary table errors.
- Most of participants used an advanced thresholding method for segmenting the CT data sets of Assembly 1 and Assembly 2.
- 5 out of 18 participants applied a software beam hardening correction during the reconstruction. 3 of the participants, who applied software beam hardening correction, did not apply physical filter on the X-ray tube.
- The investigations were all conducted in accordance with the technical protocol in terms of datum system and feature evaluations. Elementary feature such as cylinders, planes and lines were used for defining the datum system and the selected measurands for both Assembly 1 and Assembly 2.
- The majority of participants used voxel files for both Assembly 1 and Assembly 2. Some participants instead worked on STL files. No substantial difference between measurements conducted using voxel files and STL files were observed due to the almost totally absence of image artefacts within the data sets.
- Most of participants did not use the provided CAD model for alignment and evaluations. Some participants used provided CAD model in order to more easily set the measuring strategies.

The main conclusions of this comparison are outlined as follows:

- 71% of the measurements conducted using the Own Choice yielded $|E_n|$ values less than 1 for Assembly 1. The Own Choice approach did not apply any scanning restrictions on any of the

scanning parameters.

- 59% of the measurements carried out using the Fast Scan approach yielded $|E_n|$ values less than 1 for Assembly 1. The Fast Scan approach introduced a series of limitations such as the scanning time and the number of frames per projection.
- Most of the participants were able to reduce their scanning time by more than 70% without affecting the accuracy of length measurements.
- 16 of the 22 participants stated a measurement uncertainty within this comparison, with the majority of the participants below 10 µm.
- Measurements on Assembly 2 showed that increasing the complexity of the measurand increases the range of variation among participants. The definition of datum system has appeared as the major source of measurement errors.
- All the participants carried out measurements following without problems the measurement procedures distributed by the coordinator.
- All circulated samples of Physical Assembly have shown a good stability over a period of 8 months for all measurands.

6. References

[Technical Protocol]	A. Stolfi, L. De Chiffre, InteraqCT comparison on assemblies, Technical Protocol, Department of Mechanical Engineering, Technical University of Denmark, 2016.
[Reference Measurements]	A. Stolfi, L. De Chiffre,InteraqCT comparison on assemblies, Reference Measurements, Department of Mechanical Engineering, Technical University of Denmark, 2016.
[ISO/IEC 17043, 2010]	ISO/IEC 17043:2010, Conformity assessment, General requirements for proficiency testing.
[ISO/IEC Guide 98-3, 2008]	ISO/IEC Guide 98-3, 2008, Uncertainty of measurement -- Part 3: Guide to the expression of uncertainty in measurement.

7. Appendix

InteraqCT comparison on assemblies

Measurement report for Assembly 1 by fast scan

GENERAL INFORMATION	
Participant short name	
Participant number	
Contact person	
Operator	

CT SCANNER	
Instrument type (manufacturer)	
Year	
MPE values in µm (if known)	

SOFTWARE	
Acquisition software	
Reconstruction software	
Analysis software	

PRELIMINARY ACTIVITIES (NB: if corrections applied are confidential, please indicate it)	
Scale error correction (Y/N)	
Artefact for scale error correction	
Other corrections applied	
Shading artifact correction (Y/N)	
Ring artifact reduction (Y/N)	

SETUP AND SCANNING	
Orientation of the item (+ photo)	
Hard filter: Pre-filter material and thickness in mm (if applied)	
Temperature inside scanner before and after scanning in °C	
Number of scans per item	
Voltage in kV	
Current in µA	
Power in W	
Source-detector distance in mm	
Source-object distance in mm	
Geometrical magnification	
Uncorrected voxel size in µm	
Corrected voxel size in µm	
No. of views (projections)	
Integration time in s	
No. of image averaging	
Binning	
Data set size in GB	
Scanning time in min.	

PROCESSING PARAMETERS	
Beam hardening correction (if used, what order of the function)	
Data filtering during the reconstruction (Y/N and what type of filter)	
Voxel size after scale correction in µm	
Surface determination method (threshold-based or region growing based)	
Thresholding value (if known)	
ROI during surface determination (Y/N and how many)	
Morphological operators (Y/N and what type of operator)	
Data filtering (Y/N and what type of filter)	
Analysis carried out on volume data (original voxel data) or surface data (STL)	
Post-processing time in min.	

MEASURING PROCEDURE	
Datum system for measurements as indicated in the Technical Protocol (Y/N)	
Measurements in either the 2D or the 3D window	
Modification of the measuring strategies (Y/N and what type of modification)	

UNCERTAINTY ASSESSMENT	LIST OF UNCERTAINTY CONTRIBUTORS
Method (indicate what of the following is used)	1)
1) GUM (analytical method)	2)
2) ISO 14253-2 (simplified uncertainty method)	3)
3) ISO 15530-3 (substitution method)	...
4) VDI/VDE 2617-7 (simulation)	
5) Manufacturer specifications of the CT scanner	
6) Other	

ATTACHMENTSz	Name of attachment
Photos of item and fixture on rotary table	
Raw CT data (e.g. .vgl)	
Processed CT data (e.g. .vgl)	
Other relevant information	

MEASUREMENT RESULTS All measurements are to be referred to 20°C

Measurand	Average in mm	Expanded uncertainty in mm (k=2)
L1		
L2		
L3		
L4		

Date:	

InteraqCT comparison on assemblies

Measurement report for Assembly 1 by fast scan

GENERAL INFORMATION	
Participant short name	
Participant number	
Contact person	
Operator	

CT SCANNER	
Instrument type (manufacturer)	
Year	
MPE values in µm (if known)	

SOFTWARE	
Acquisition software	
Reconstruction software	
Analysis software	

PRELIMINARY ACTIVITIES (NB: if corrections applied are confidential, please indicate it)	
Scale error correction (Y/N)	
Artefact for scale error correction	
Other corrections applied	
Shading artifact correction (Y/N)	
Ring artifact reduction (Y/N)	

SETUP AND SCANNING	
Orientation of the item (+ photo)	
Hard filter: Pre-filter material and thickness in mm (if applied)	
Temperature inside scanner before and after scanning in °C	
Number of scans per item	
Voltage in kV	
Current in µA	
Power in W	
Source-detector distance in mm	
Source-object distance in mm	
Geometrical magnification	
Uncorrected voxel size in µm	
Corrected voxel size in µm	
No. of views (projections)	
Integration time in s	
No. of image averaging	
Binning	
Data set size in GB	
Scanning time in min.	

PROCESSING PARAMETERS	
Beam hardening correction (if used, what order of the function)	
Data filtering during the reconstruction (Y/N and what type of filter)	
Voxel size after scale correction in µm	
Surface determination method (threshold-based or region growing based)	
Thresolding value (if known)	
ROI during surface determination (Y/N and how many)	
Morphological operators (Y/N and what type of operator)	
Data filtering (Y/N and what type of filter)	
Analysis carried out on volume data (original voxel data) or surface data (STL)	
Post-processing time in min.	

MEASURING PROCEDURE	
Datum system for measurements as indicated in the Technical Protocol (Y/N)	
Measurements in either the 2D or the 3D window	
Modification of the measuring strategies (Y/N and what type of modification)	

UNCERTAINTY ASSESSMENT	LIST OF UNCERTAINTY CONTRIBUTORS
Method (indicate what of the following is used)	1)
1) GUM (analytical method)	2)
2) ISO 14253-2 (simplified uncertainty method)	3)
3) ISO 15530-3 (substitution method)	...
4) VDI/VDE 2617-7 (simulation)	
5) Manufacturer specifications of the CT scanner	
6) Other	

ATTACHMENTSz	Name of attachment
Photos of item and fixture on rotary table	
Raw CT data (e.g. .vgi)	
Processed CT data (e.g. .vgl)	
Other relevant information	

MEASUREMENT RESULTS All measurements are to be refered to 20°C

Measurand	Average in mm	Expanded uncertainty in mm (k=2)
L1		
L2		
L3		
L4		

Date:	

InteraqCT comparison on assemblies
Measurement report for Assembly 2 using CT data set

GENERAL INFORMATION	
Participant short name	
Participant number	
Contact person	
Operator	

SOFTWARE	
Acquisition software	
Reconstruction software	
Analysis software	

PROCESSING PARAMETERS	
Beam hardening correction (if used, what order of the function)	
Data filtering during the reconstruction (Y/N and what type of filter)	
Surface determination method (threshold-based or region growing based)	
Thresolding value (if known)	
ROI during surface determination (Y/N and how many)	
Morphological operators (Y/N and what type of operator)	
Data filtering (Y/N and what type of filter)	
Analysis carried out on volume data (original voxel data) or surface data (STL)	
Post-processing time in min.	

MEASURING PROCEDURE	
Datum system for measurements as indicated in the Technical Protocol (Y/N)	
Measurements in either the 2D or the 3D window	
Modification of the measuring strategies (Y/N and what type of modification)	

ATTACHMENTS	Name of attachment
Processed CT data (e.g. .vgl)	
STL files (if relevant)	
Other relevant information	

MEASUREMENT RESULTS

Measurand	Average in mm	standard deviation in mm
Diameter D1		
Diameter D2		
Roundness R2		
Concentricity C1		

Date:	

E-mail to: alesto@mek.dtu.dk

InteraqCT comparison on assemblies
Measurement report for Assembly 2 using stack of X-ray images

GENERAL INFORMATION	
Participant short name	
Participant number	
Contact person	
Operator	

SOFTWARE	
Acquisition software	
Reconstruction software	
Analysis software	

PROCESSING PARAMETERS	
Beam hardening correction (if used, what order of the function)	
Data filtering during the reconstruction (Y/N and what type of filter)	
Surface determination method (threshold-based or region growing based)	
Thresolding value (if known)	
ROI during surface determination (Y/N and how many)	
Morphological operators (Y/N and what type of operator)	
Data filtering (Y/N and what type of filter)	
Analysis carried out on volume data (original voxel data) or surface data (STL)	
Post-processing time in min.	

MEASURING PROCEDURE	
Datum system for measurements as indicated in the Technical Protocol (Y/N)	
Measurements in either the 2D or the 3D window	
Modification of the measuring strategies (Y/N and what type of modification)	

ATTACHMENTS	Name of attachment
Processed CT data (e.g. .vgl)	
STL files (if relevant)	
Other relevant information	

MEASUREMENT RESULTS		
Measurand	Average in mm	standard deviation in mm
Diameter *D1*		
Diameter D2		
Roundness R2		
Concentricity C1		

Date:	

E-mail to: alesto@mek.dtu.dk